NASA

Technical Memorandum 83832

Equatorial Superrotation in a Thermally Driven Zonally Symmetric Circulation

H. G. Mayr and I. Harris

SEPTEMBER 1981

National Aeronautics and
Space Administration

Goddard Space Flight Center
Greenbelt, Maryland 20771

EQUATORIAL SUPERROTATION IN A THERMALLY DRIVEN ZONALLY SYMMETRIC CIRCULATION

by

H. G. Mayr and I. Harris

Laboratory for Planetary Atmospheres

Goddard Space Flight Center

Greenbelt, MD 20771

September 1981

Presented at the AGU meeting, EOS, 62, 314, 1981 and IAGA Scientific Assembly, Edingurgh, IAGA Bulletin, 45, 471, 1981.

ABSTRACT

The perception has been that the equatorial jets observed on Jupiter and Saturn cannot be understood in the framework of a zonally symmetric circulation; that some kind of eddy process equivalent to upgradient diffusion with negative viscosity is required to accelerate the motions. We arrive at a different conclusion when we examine this problem with spectral models describing a viscous fluid. Near the equator where the Coriolis force vanishes, the momentum balance is established between horizontal and vertical diffusion, which, a priori, does not impose constraints on the direction or magnitude of the zonal winds. Solar radiation absorbed at low latitudes is a major force in driving large scale motions with air rising near the equator and falling at high latitudes. In the upper leg of the meridional cell, angular momentum is redistributed so that the atmosphere tends to subrotate (or corotate) at low latitudes and superrotate at high latitudes. In the lower leg, however, the process is reversed and produces a tendency for the equatorial region to superrotate. The outcome depends on the energy budget which is closely coupled to the momentum budget through the thermal wind equation; a pressure (temperature) maximum is required to sustain equatorial superrotation. Such a condition arises in regions which are convectively unstable and the temperature lapse rate is superadiabatic. It should arise in the tropospheres of Jupiter and Saturn; planetary energy from the interior is carried to higher altitudes where radiation to space becomes important. Upward equatorial motions in the direct and indirect circulations (Ferrel-Thomson type) imposed by insolation can then "trap" dynamic energy for equatorial heating to sustain the superrotation of the equatorial region. Due to vertical momentum diffusion and convection the dynamic signatures from the troposphere and lower stratosphere are "mixed" and produce a complex

interference pattern in the zonal circulation near the tropopause. We attribute the large differences between the circulations on Jupiter and Saturn to differences in size, gravitational acceleration, temperature, eddy diffusivity, and tropospheric stability.

INTRODUCTION

Atmospheric superrotation is observed on virtually every planet in our solar system (e.g. King-Hele, 1964; Conrath et al., 1973; Smith et al., 1979a,b; Alexander, 1962; Schubert et al., 1980). In each case, the planet's rotation axis is nearly perpendicular to the orbital plane around the Sun, the equatorial region is heated preferentially and its pressure decreases toward higher latitudes. Applying the concepts of geostrophic and cyclostrophic equilibria, reasonably small latitudinal pressure gradients (order of $\frac{1}{p}\frac{\partial p}{\partial \Theta} \sim 0.3$) can account for the wide range of superrotation rates that are observed. On the basis of this evidence, we are led to believe that thermal forcing (e.g. Lorenz, 1967; Leovy, 1973; Gierasch, 1975) is a major if not the prime candidate for driving atmospheric superrotation.

In an earlier paper (Mayr and Harris, 1981) we had considered the angular momentum budget of a thermally driven zonally symmetric circulation and provided an elementary description of the processes leading to and maintaining the rigid shell component of superrotation. It was shown that depending on the transport properties, an atmosphere can go through two different modes. For large viscosity it behaves almost like a solid body, frictionally coupled to the planet. The angular momentum for superrotation is then "derived" from the decrease in the moment of inertia due to mass redistribution by the meridional circulation; during the "spin up time" the atmosphere transfers angular momentum to the planet. For lower and more realistic values of viscosity there is an important additional degree of freedom in the vertical momentum distribution. Mass can more freely return from the poles in the lower leg of the meridional cell and the change in the moment of inertia is not as large. This return flow together with the increased tendency toward geostrophy causes subrotation in the lower regions of the atmosphere during the initial phase of the spin up process. Through viscous shear the planet applies a torque to the atmosphere which propagates upwards and in time supplies the angular momentum for large superrotation. Thus in steady state, under thermal forcing, a rigid shell component of superrotation eventually prevails at all altitudes.

A longstanding and remaining problem is differential rotation. Outstanding examples are the banded wind fields and the very large well defined equatorial jets on Jupiter (e.g. Smith et al., 1979a,b) and Saturn (Smith et al., 1981) which are not understood.

The general perception is that equatorial superrotation cannot develop in a thermally driven zonally symmetric circulation (e.g., Hide, 1969, 1971; Gierasch, 1975; Held and Hou, 1980). Large scale eddy processes are therefore invoked to explain the observations. For Jupiter it is estimated (Ingersoll, 1981) that eddies ranging in size from 100 to 1000 km contain enough energy to accelerate the prevailing zonal circulation within a short period of one month, giving credence to the notion that, somehow, "order comes out of chaos."

We suggest in this paper, contrary to current theory, that the equatorial jets on Jupiter and Saturn <u>can</u> be understood in the framework of a thermally driven zonally symmetric circulation. First, an empirical model is presented for Jupiter's zonal wind field observed by the Voyager spacecraft. The power spectrum in terms of vector spherical harmonics conveys a very simple and beautiful order, in which momentum can be perceived to cascade from lower to higher order modes. Second, the theorem of equatorial subrotation (e.g., Hide, 1969; Held and Hou, 1980) is critically examined and an alternative interpretation is presented. Near the equator where the Coriolis force vanishes, the momentum balance is established between horizontal and vertical diffusion, which, a priori, does not impose constraints on the direction or magnitude of the zonal winds. Thus, the problem is reduced to explain how momentum and energy are transported into the equatorial region? Third, a spectral model and the concept of mode coupling are introduced to describe the direct and indirect circulations driven by the absorption of solar radiation at low latitudes. Fourth, the momentum and energy budgets are qualitatively discussed for the meridional circulation driven by solar differential heating. Relative to the rigid shell component of superrotation which receives most of its angular momentum from the planet during spin up, angular momentum is redistributed in the upper leg of the meridional cell so that the atmosphere tends to subrotate or corotate at low latitudes and superrotate at high latitudes. In the lower leg, however, the process is reversed and a tendency for the equatorial region to superrotate is produced. Whether this actually occurs depends crucially on the energy budget which is closely coupled to the momentum budget through the thermal wind equation; a pressure (temperature) maximum is required to sustain equatorial superrotation. The necessary condition for this should arise in the tropospheres of Jupiter and Saturn, where small scale convection must transport energy from the interior upwards, and therefore the temperature lapse rate should be superadiabatic. Upward equatorial motions in the direct and indirect circulations (of the Ferrel-Thomson type), induced by insolation, can then "trap" or "focus" dynamic energy for equatorial heating which is required to sustain equatorial superrotation. Fifth, using parameterizations in terms of Newtonian cooling and Raleigh friction, simple analytical solutions for the spectral model are presented which elucidate some basic properties of the zonal circulation in different regimes of the atmosphere and under different planetary conditions. Sixth, allowing for molecular and eddy transport processes, including vertical and horizontal momentum diffusion in the meridional and zonal force balances, a numerical solution is presented which describes equatorial superrotation in a zonally symmetric circulation driven by solar differential heating. Angular momentum is thereby allowed to cascade from lower order modes where most of the energy is absorbed to higher order modes. The integration is carried out from the lower troposphere (25 bar pressure) up into the exosphere.

OBSERVATIONS

Spectral analyses of the zonal wind field on Jupiter observed by the Voyager Spacecraft (G. Hunt, private communication) are shown in Figure 1. They are based on empirical representations of the data in terms of vector spherical harmonics which also serve as basis functions for our theoretical model (Mayr and Harris, 1981). The amplitudes in the lower part of Figure 1 are the equatorial values of the solenoidal harmonics $\vec{C}_{\ell-1}$ (Morse and Feschbach, 1953). Positive and negative values contribute to superrotation and subrotation at the equator respectively. In the upper part of Figure 1 analytical representations of the Voyager I data from both hemispheres are presented for syntheses up to order L=12 and 34. Included are only the harmonics which are symmetrical with respect to the equator (even wave number ℓ).

The fundamental harmonic (ℓ=2) or the rigid shell component of superrotation dominates. Higher order modes, ℓ>4, are at least a factor of two smaller and are apparently in a separate class of their own. After the abrupt decrease between ℓ=2 and ℓ=4 the amplitudes decrease gradually and monotonically toward higher wave numbers. Near ℓ=18 the sign changes, and the spectrum up to ℓ=30 contributes to equatorial subrotation. We note that the spectra for the Voyager I and II observations are nearly identical.

Anticipating the theoretical results discussed later on we offer the following interpretation. The rigid shell component of superrotation (ℓ=2) is primarily driven by differential heating from solar radiation where most of the energy is deposited in the lowest order harmonics (e.g., Voliand and Mayr, 1972a). We refer to it as "direct circulation". That component receives most of its angular momentum from the planet or the planetary interior during spin up (Mayr and Harris, 1981). In contrast, the solar input into the higher order modes is relatively small and "direct forcing" is probably not important. This part of the circulation spectrum is excited by mode coupling in which momentum (and energy), originating primarily in the solar driven rigid shell component of superrotation, cascade from lower to higher order modes. We refer to it as "indirect circulation".

For vector spherical harmonics, the Coriolis force induces mode coupling; the range of momentum transfer in ℓ space being proportional to the planetary rotation rate. By comparison with the global scale circulation on Venus, a slowly rotating planet, the zonal velocity fields on Jupiter and Saturn are therefore confined into narrow latitude bands. From the synthesis in Figure 1 one can see that the lower order harmonics (L=12) primarily contribute to the equatorial jet, supporting our interpretation that solar radiation absorbed in the lowest order harmonics is driving these motions. We attribute equatorial superrotation to momentum advection in the lower leg of the meridional cell and energy convection into the region below the cloud top, where, presumably, the temperature lapse rate is superadiabatic. The negative (equatorial) velocities in the power spectrum around ℓ=22 are largely responsible for the positive jet near 25° latitude. We believe that this feature is the signature of poleward momentum and energy transport in the upper leg of the meridional cell. The effect is not (or to a much lesser extent) seen on Saturn (Smith et al., 1981), indicating that the clouds form at a lower altitude deep inside the (unstable) convection region, consistent with the lower temperatures observed on this planet (Hanel et al. 1981).

DIFFUSION : LARGE SCALE CIRCULATION

Assuming $|U| << |\omega_p r|$, the conservation of angular momentum with respect to the planetary rotation axis can be expressed as

$$\vec{\nabla}\cdot(\vec{V} M_o) = \frac{\partial}{\partial r}\frac{\eta_r}{m}\left[\frac{\partial \Delta M}{\partial r} + \frac{\Delta M}{H}\right] + (F_\theta) \tag{1}$$

where

$\vec{V}$ = (U, V, W), wind vector with zonal, meridional and vertical components

M_o = $\omega_p r^2 \rho_o \cos^2\Theta$, "planetary" angular momentum of the atmosphere

ΔM = $U r \rho_o \cos\Theta$, atmospheric angular momentum

F_Θ = $\frac{\eta_\theta \rho_o}{m}\frac{\partial^2}{\partial \theta^2}\left(\frac{U}{r\cos\theta}\right)$, momentum diffusion (viscous flow) due to meridional shear

ρ_o, global average of mass density,

H, density scale height,

m, mass

η_r, η_Θ, viscosity coefficients in the vertical or horizontal directions,

ω_ρ, planetary angular velocity

r, radial distance from the center of the planet

Θ latitude

From the continuity of mass flow, $\vec{\nabla}\cdot(\vec{V}\rho_o) = 0$, the left hand side of (1) reduces to $\vec{\nabla}\cdot(\vec{V}M_o) = 2\omega_p r V \rho_o \sin\Theta\cos\Theta$ which vanishes at the equator.

Following Held and Hou (1980), the assumption is made that $F_\Theta = 0$. Since $U=0$ at the planetary surface and $\frac{\partial U}{\partial r} = 0$ at the top of the atmosphere, it follows that

$$U\ (r) = U\ (\text{equator}) \tag{2}$$

at all altitudes.

A parcel of air moving in a Hadley cell from the equator toward the pole is accelerated under conservation of angular momentum giving rise to superrotation. Nowhere along the trajectory can the total angular momentum, $M_T = M_o + \Delta M$, exceed the planetary angular momentum at the equator (Eq. 2). This is an upper limit considering viscous dissipation, and it follows

$$U < \frac{\omega_p r \sin^2\Theta}{\cos\Theta} \quad . \tag{3}$$

Equation (3) is due to Hide (1969) and expresses a fundamental theorem of atmosphere dynamics. Considering the constraint (Eqs. 2 and 3) on the zonally symmetric circulation, Hide (1969), Held and Hou (1980), Ingersoll et al. (1979) and others concluded that eddy processes, equivalent to upgradient diffusion with negative horizontal viscosity, must provide the angular momentum for the equatorial accelerations on Jupiter and Saturn.

We question here the general validity of Hide's theorem (Eq. 3). By neglecting horizontal momentum diffusion ($F_\theta = 0$) in (1), only the Coriolis force remains to balance vertical diffusion, and that balance breaks down near the equator, producing the trivial result that the atmosphere must corotate (2). But given the physical reality of horizontal diffusion, all that can be said about the equator is that horizontal influx or outflux of momentum must be balanced by vertical outflux or influx of momentum, respectively. A priori, under this force balance, there is no constraint on the direction or magnitude of the zonal wind velocity; the atmosphere is permitted either to subrotate or superrotate at the equator. A good example is the observed wind field on Jupiter (Figure 2). At latitudes below about 7^{o}, angular momentum is diffusing downgradient toward the equator where it can be carried through vertical shears to lower and or higher altitudes. This being true, the question reduces to how angular momentum is transported into or out of the "equatorial region" (Figure 2)?

We assume that solar radiation preferentially absorbed at low latitudes supplies the energy for the thermally driven meridional circulation with air rising near the equator and falling at higher latitudes. Under conservation of mass, more planetary angular momentum is carried upward by vertical motions at low latitudes than is descending at high latitudes. This global inbalance is compensated by downward diffusion or viscous flow (e.g., Leovy, 1973; Gierasch, 1975) which requires the atmosphere to assume a global average or rigid shell component of superrotation all the way down to the surface (Figure 3). The angular momentum is supplied primarily from the planet during spin up. Given that basic component, the question is what are the characteristics of differential rotation related to differential (equatorial) heating?

MOMENTUM AND ENERGY BALANCE

In answering these questions we present first an idealized and heuristic interpretation of equatorial superrotation. At altitudes above the center of the meridional circulation, where the heat input per mass is relativiely large, angular momentum is effectively advected poleward, except in the "equatorial region" where the meridional winds and the Coriolis force go to zero and the horizontal momentum transport must be carried by horizontal diffusion. This causes the atmospheric rotation rate, relative to the rigid shell component of superrotation, to decrease (minus) at low latitudes and increase (plus) at high latitudes (Figure 4). The equatorial region therefore tends to corotate or subrotate, consistent with Hide's theorem (Eq. 3). Below the center of the meridional circulation the process is reversed. Angular momentum is advected from high to low latitudes so that, relative to the rigid shell component of superrotation, the rotation rate tends to decrease at high latitudes and increase at low latitudes (Figure 4). Again, in the vicinity of the equator, it is understood that the momentum transport is taken over by horizontal diffusion.

However, this picture is not unique as demonstrated in the upper part of Figure 5. Three different velocity distributions are shown which can balance, through vertical diffusion, the momentum advection into and out of the equatorial region in the upper and lower legs of the meridional cell. At the planetary surface or deep inside the atmosphere the velocity is assumed to be zero. For case (b) the zonal velocities are positive (superrotation) and negative (subrotation) at lower and higher altitudes, respectively, representing the scenario described in Figure 4. But for (a) and (c) the atmosphere superrotates and subrotates at all altitudes.

Whether the redistribution of angular momentum by the meridional circulation actually leads to superrotation or subrotation crucially depends on the energy budget which is closely coupled to the momentum budget through the thermal wind equation. Applying perturbation theory, we consider the conservation of energy in simplified form

$$(\alpha - \kappa_r \frac{\partial^2}{\partial r^2}) \Delta T + c_p W (\frac{\partial T_o}{\partial r} + \Gamma) = \Delta Q \qquad (4)$$

where

c_p, specific heat per mass at constant pressure

α, coefficient of radiative cooling,

κ_r, thermal conductivity per unit mass

W, vertical velocity

T_o, average temperature

ΔT, temperature perturbation

Γ, adiabatic lapse rate

ΔQ, energy input per unit mass

For the indirect circulation ($\Delta Q = 0$), the temperature perturbation is determined by energy convection due to vertical motions

$$\Delta T = \frac{-c_p W(\frac{\partial T_o}{\partial r} + \Gamma)}{(\alpha - \kappa_r \frac{\partial^2}{\partial r^2})} \quad . \tag{5}$$

Under "local" conditions it is reasonable to assume $\kappa_r \frac{\partial^2}{\partial r^2} < 0$.

Normally, with static stability $(\frac{\partial T_o}{\partial r} + \Gamma) > 0$, the upward motions ($W > 0$) near the equator cause the temperature to decrease, $\Delta T < 0$. Through the thermal wind equation, the resulting pressure decrease tends to produce subrotation, and case (c) in Figure 5 describes the momentum budget. This condition applies to the atmosphere at higher altitudes.

However, when the temperature lapse rate is superadiabatic, $(\frac{\partial T_o}{\partial r} + \Gamma) < 0$, the indirect meridional circulation is capable of "trapping" dynamic energy convected upwards from lower altitudes (Figure 5). The temperature then increases, $\Delta T > 0$, and the accompanying pressure maximum permits superrotation in the equatorial region. Such a condition arises in regions of the atmosphere which are characterized by global scale energy diffusion to higher altitudes where radiation to space is important. On Venus this is observed below the visible cloud top, between 50 and 60 km. It should also arise in the tropospheres of Jupiter and Saturn where energy from the planetary interior is carried upwards by small scale convection. To a much lesser extent, it may also arise in the troposphere on Earth.

In summary, we emphasize some subtle points which are important to understand equatorial superrotation:

(a) Balancing vertical momentum diffusion with Coriolis force, when applied to the equator, led to an unphysical constraint on the zonal wind velocity (Eq. 2). With the reality of horizontal diffusion, this process may or may not be important in various regions of the atmosphere. But it is certain that horizontal diffusion must be important near the equator. The vanishing Coriolis force on its own cannot provide a balance for vertical diffusion which is known to play a major part in the global momentum budget. With the inclusion of horizontal diffusion, there is no constraint on the direction or magnitude of the equatorial zonal wind velocity.

(b) Under the constraint (2), the tacit assumptions were made that the meridional motions carry angular momentum from the equator toward the poles (only), and that in this process angular momentum is (always) lost through diffusion; the consequence of the argument was Hide's theorem (3). At higher altitudes where the specific heat input is relatively large, it is indeed reasonable to assume that the meridional motions are directed away from the equatorial source and that dissipative processes due to diffusion would tend to dampen the zonal wind velocities. However, in the lower leg of the meridional circulation where the return flow occurs, this process is reversed. The motions are directed toward the equator. Angular momentum diffusing downwards from higher altitudes can be picked up and transported to lower latitudes which would tend to accelerate the equatorial region. A factor contributing to this problem may have been the neglect of viscous momentum transfer in the meridional force balance. Under that simplifying assumption the meridional velocities cannot be forced to vanish, as they should, at the planetary surface. Thus an excessive amount of the momentum return flow is confined to the lowest altitudes where the zonal velocities must vanish.

(c) Finally, the picture of a fluid being spun up by poleward motions under conservation of angular momentum was incomplete for another reason, the most important one perhaps. While vertical diffusion was considered with the inclusion of dissipation, momentum and energy convection by the vertical motions in the meridional circulation did not play a part in Hide's theorem (3). Yet we know that this transport process is important in supplying the atmosphere with angular momentum from the vast reservoir of the planet; computer simulations of the spin up in which the average or rigid shell component of superrotation is established clearly demonstrate its importance (Mayr and Harris, 1981). Within the atmosphere that angular momentum is then redistributed by the indirect circulation, and the upward motions at the equator play again an important part. In regions of the atmosphere, below radiating cloud-or haze-layers where the temperature lapse rate can be superadiabatic, energy convection from below increases the temperature (and pressure). This is turn provides the basis, energetically, for accelerating the equatorial region directly, or indirectly due to vertical expansion and diffusion which can carry angular momentum to higher altitudes.

MODEL AND MODE COUPLING

To describe differential rotation we adopt a spectral model (Mayr and Volland, 1972; Harris and Mayr, 1975; Mayr et al., 1978; referred to as MH). Its properties relevant for our analysis are briefly summarized: (1) Advection and convection of energy, mass and momentum associated with the large scale zonally symmetric circulation are considered. (2) Vertical and horizontal diffusion of energy and momentum (in both the zonal and meridional force balances) are included. (3) Perturbation theory is applied relative to a globally uniform atmosphere which corotates with the underlying planet; the physical variables such as temperature, density and wind vector are expanded in terms of spherical harmonics (with the zonal wave number being zero) which effectively separate latitude from altitude variations. (4) Using tridiagonal block elimination, the resulting set of difference equations are solved from the planetary surface (or atmospheric interior) up to the exosphere. (5) At the lower boundary, the vertical, meridional and zonal velocities as well as the density and temperature variations are set to zero. For the upper boundary conditions, the dominance of molecular diffusion requires that the vertical gradients of temperature and horizontal winds vanish.

No separable eigen functions exist to describe the latitude dependence for the prevailing atmospheric circulation. Hough modes are appropriate eigen functions only when dissipative processes due to viscosity can be neglected (Chapman and Lindzen, 1968), and spherical harmonics are appropriate only when the Coriolis force is unimportant (Volland and Mayr, 1972b). Neither of these conditions is satisfied, and mode coupling must be considered.

For a set of basis functions, chosen to be spherical harmonics, this implies that an external source in one spherical harmonic "mode" not only excites an atmospheric perturbation in that particular mode; it also excites, to various degrees, all the other modes. Given a latitudinal distribution of the source, the structure of the atmospheric response changes depending on the importance of mode coupling, and one of the principle determining factors in that is the planetary rotation rate (Coriolis force).

Since individual modes are coupled together, their definition should, in principle, not affect the solution as long as the set of basis functions is complete and the expansion includes a sufficiently large number of terms. For mathematical convenience we chose "P_ℓ modes" of order ℓ each defined by a set of (vector) spherical harmonics (P_ℓ, $\vec{B}_\ell$, $\vec{C}_{\ell-1}$; Morse and Feschbach, 1953)

$$\left.\begin{matrix} \Delta Q \\ \Delta T \\ \\ \Delta \log p \\ W \end{matrix}\right\} = \sum_{\ell=2,4\ldots}^{N} (-1)^{\ell/2} x_\ell (r) P_\ell (\Theta) \tag{6}$$

$$\vec{V} = \sum_{\ell=2,4\ldots}^{N} (-1)^{\ell/2} V_\ell (r) \vec{B}_\ell \tag{7}$$

$$\vec{J} = \sum_{\ell=2,4\ldots}^{N} (-1)^{(\ell/2+1)} U_{\ell-1} (\vec{r}) C_{\ell-1} \tag{8}$$

where $\Delta \log p$ is the logarithm of the pressure ratio (disturbed to undisturbed). For even ℓ values the circulation is symmetrical with respect to the equator. The amplitudes in (6), (7) and (8) are so defined that, arbitrarily close to the equator, positive amplitudes $\left[x_\ell (r), V_\ell (r), U_{\ell-1} (r)\right]$ give positive contributions to the physical variables such as $\Delta T (r, \Theta)$, $\vec{V} (r, \Theta)$ and $\vec{U} (r, \Theta)$.

With this ansatz the equations of energy, mass and momentum conservation take the form

$$\left(\alpha + \frac{\ell(\ell+1)}{r^2} \kappa_\Theta - \kappa_r \frac{\partial^2}{\partial r^2}\right) \Delta T_\ell + c_p W_\ell \left(\frac{\partial T_o}{\partial r} + \Gamma\right) = q_\ell \tag{9}$$

$$\frac{W_\ell}{H} - \frac{\partial W_\ell}{\partial r} + \frac{\sqrt{\ell(\ell+1)}}{r} V_\ell = 0 \tag{10}$$

$$\frac{\partial}{\partial r} \Delta \log p_\ell - \frac{mg}{kT_o^2} \Delta T_\ell = 0 \tag{11}$$

$$\omega m\, f(\ell)\, U_{\ell-1} - \left(\frac{\ell(\ell+1)}{r^2} \eta_\theta - \eta_r \frac{\partial^2}{\partial r^2}\right) V_\ell - \frac{\sqrt{\ell(\ell+1)}}{r} kT_o\, \Delta \log p_\ell$$
$$= \omega m\, f(\ell + 1)\, U_{\ell+1} \tag{12}$$

$$\omega m\, f(\ell)\, V_\ell + \left(\frac{\ell(\ell-1)}{r^2} \eta_\Theta - \eta_r \frac{\partial^2}{\partial r^2}\right) U_{\ell-1} = \omega m\, f(\ell-1)\, V_{\ell-1} \tag{13}$$

where g is the gravitational acceleration and

$$f(\ell') = \frac{2}{(\ell'+1)} \sqrt{\frac{\ell'(\ell'+2)(\ell'+1)^2}{(2\ell'+1)(2\ell'+3)}} \sim 1 \tag{14}$$

For brevity, we are omitting here a number of terms involving vertical and horizontal energy and momentum diffusion. In the lowest order mode, for example, the horizontal momentum flux should vanish. The complete expressions are considered in our numerical analysis.

The equations (9 through (14) describe the P_ℓ mode in the context of a larger system schematically illustrated in Figure 6. On the right hand side of (12) and (13) are the momentum sources due to mode coupling which arise from the Coriolis force and involve the adjacent modes.

To simplify the discussion, we assume that the atmospheric circulation is forced only with the lowest order heat source

$$\Delta Q_2 = -q_2\,(r)\; P_2\,(\theta)$$
$$\Delta Q_\ell = 0, \text{ for } \ell > 2, \tag{15}$$

representing differential heating by solar radiation which is preferentially absorbed at low latitudes.

In an earlier paper (Mayr and Harris, 1981) we discussed some characteristics of the fundamental P_2 mode or the rigid shell component of superrotation which is directly driven by the solar input (15). This mode is unique in that its global angular momentum and moment of inertia do not vanish. During spin up, that angular momentum is primarily supplied by the planetary torque at the surface and is transported to higher altitudes through viscous shears and the meridional circulation. In contrast to the fundamental mode, the global angular momentum and moment of inertia of the higher order modes $P_\ell(\ell>2)$, describing differential rotation, are identically zero, and the problem is no longer where the angular momentum for superrotation comes from but how it is redistributed within the atmosphere?

Later on a numerical soluton of the differential equations (9) through (13) will be presented in which we consider in self consistent form the mode (momentum) coupling originating from the lowest order heat source (15).

QUALITATIVE ANALYSIS

The vertical structure of the atmospheric circulation is parameterized

$$-\kappa_r \frac{\partial^2 \Delta T_\ell}{\partial r^2} = C_\kappa \, \Delta T_\ell \tag{16}$$

$$-\eta_r \frac{\partial^2 U_{\ell-1}}{\partial r^2} = C_\eta U_{\ell-1} \tag{17}$$

$$\Delta \log p_\ell = \frac{mg}{k} \frac{h}{T_o^2} \Delta T_\ell \tag{18}$$

$$W_\ell = \pm\sqrt{\ell(\ell+1)} \, \frac{h}{r} \, |V_\ell| \tag{19}$$

where the sign of W_ℓ is determined by the sign of V_ℓ in the lower leg of the meridional circulation. h is a measure for the vertical extent of the circulation, and is positive.

Since thermal forcing by solar radiation is only considered in the lowest order mode (15), it is reasonable to assume, that, in the process of cascading momentum to higher order modes, the zonal and meridional wind components would tend to decrease

$$U_{\ell-1} - U_{\ell+1} = U_{\ell-1}(1 - \beta) \tag{20}$$

$$V_{\ell-2} - V_\ell = V_\ell \, (1 - \beta) \tag{21}$$

The parameter $0 < \beta < 1$ vanishes as mode coupling ceases to be important.

Substituting (16) through (21) and ignoring momentum diffusion in (12), the equations (9) through (14) take the form

$$(\alpha + \frac{\ell(\ell+1)}{r^2} \kappa_\Theta + C_\kappa)\Delta T_\ell \pm \sqrt{\ell(\ell+1)} \, \frac{h}{r} \, c_p \, (\frac{\partial T_o}{\partial r} + \Gamma) \, |V_\ell| = q_\ell \tag{22}$$

$$\frac{\sqrt{\ell(\ell+1)}}{r} \frac{ng}{T_o} h \, \Delta T_\ell = \omega m(U_{\ell-1} - U_{\ell+1}) \sim \omega m(1-\beta)U_{\ell-1} \tag{23}$$

$$\begin{aligned} (\frac{\ell(\ell+1)}{r^2} \eta_\Theta + C_\eta) \, U_{\ell-1} &= \omega m \, (V_{\ell-2} - V_\ell) \sim \omega m(1-\beta) \, V_\ell \quad \text{for } \ell \neq 2 \\ &= -\omega m \, V_\ell \quad \text{for } \ell = 2 \end{aligned} \tag{24}$$

The equations (22) and (24) describe the conservation of energy and angular momentum respectively, and the thermal wind equation (23) describes the coupling between energy and angular momentum. To first approximation (23) does not involve diffusion processes and is therefore more "rigid" than (22) or (24), where C_κ or C_η can be either positive or negative. Normally, unless specified otherwise, it is reasonable to assume that local conditions prevail and

$$\left.\begin{array}{c} C_\kappa \\ C_\eta \end{array}\right\} > 0. \quad (25)$$

For the lowest order mode, $\ell=2$, the heat source $q_2>0$ causes the temperature to increase at the equator $\Delta T_2>0$. Equation (23) then yields the rigid shell component of superrotation, $U_1>0$, which is consistent with the momentum balance (24) for meridional winds flowing away from the equator ($V_2<0$) in the upper leg of the circulation. In the lower leg of the circulation the direction of the meridional winds is reversed. But the rigid shell component is unique in that, in steady state, it cannot exchange angular momentum with the planet. To satisfy this constraint, the vertical flux of momentum must approach zero near the lower boundary requiring that the sign of the curvature (17) must change ($C_\eta<0$). Consistent with the energy and momentum balances, a rigid shell component of superrotation thus prevails all the way down to the planet (Figure 7a).

For $\ell>2$ and $q_\ell = 0$, the situation is different. In such an "indirect circulation" the motions are driven through momentum coupling between adjacent modes, and the temperature variations ΔT_ℓ arise from dynamic heating. Moreover, for higher order modes there is no constraint on the viscous stress at the lower boundary, $(\frac{\partial U_{\ell-1}}{\partial r}) \neq 0$. We consider the indirect circulation to be forced by solar (equatorial) heating in the lowest order mode, $q_2>0$. At low latitudes the meridional winds in the lower leg of the cell are then directed toward the equator, and the positive sign applies in Equation (22).

The single most important factor determining the dynamics is the term $S_o = \frac{\partial T_o}{\partial r} + \Gamma$ in the energy balance which is also a measure for the stability of the atmosphere. With $S_o>0$ the atmosphere is convectively stable, the temperature lapse rate is subadiabatic and, in the global average, heat is diffusing downwards. Conversely, with $S_o<0$ the atmosphere is unstable, the lapse rate is superadiabatic and thermal energy is diffusing upwards.

$\underline{S_o(r) = \frac{\partial T_o}{\partial r} + \Gamma > 0}$: This condition holds, when, above r, the atmosphere absorbs more radiative energy than it emits. It usually applies to the more tenuous regions at higher altitudes, far away from the heat dissipation by the planet, where the solar radiation is less attenuated and collisional excitation is less effective. With $q_\ell=0$, the upward motions at the equator then cause the temperature to decrease, $\Delta T_\ell<0$ (22), and (23) requires that the zonal wind component also decreases ($U_{\ell-1}<0$) relative to the rigid shell component of superrotation. This is consistent with poleward transport of angular momentum in the upper leg of the circulation (24). The return flow of angular momentum toward the equator in the lower leg of the cell, however, tends to increase the zonal velocity so that its curvature must change sign ($C_\eta<0$), fulfilling force balance (24). Such a scenario is illustrated in Figure 7b.

$\underline{S_o(r) = \frac{\partial T_o}{\partial r} + \Gamma < 0}$: This condition holds when, above r, the atmosphere emits more radiative energy than it absorbs. It usually applies to the denser regions at lower altitudes, close to the heat dissipation by the planet, where the solar radiation is more attenuated and collisional excitation is more effective. With $q_\ell=0$, the upward motions at the equator cause the temperature then to increase, $\Delta T_\ell>0$ (22), and (23) requires that the zonal wind component also increases ($U_{\ell-1}>0$) relative to the rigid shell component of superrotation. This is consistent with the equatorward return flow of angular momentum in the lower leg of the circulation (24). In the upper leg of the cell, however, angular momentum is transported away from the equator which tends to decrease the zonal velocity to the extent that its curvature must change sign ($C_\eta<0$), fulfilling force balance (24). Such a scenario is illustrated in Figure 7c.

<u>$S_o(r)<0$ (lower altitudes) and $S_o(r)>0$ (higher altitudes)</u>: Under realistic conditions it is reasonable to assume that planetary atmospheres are convectively stable with subadiabatic lapse rates at higher altitudes and that they would tend to be convectively unstable with superadiabatic lapse rates at lower altitudes. For such a scenario, the circulation is then a combination of the two earlier examples and its structure near the equator is illustrated in Figure 7d. At lower altitudes, below the tropopause ($S_o<0$), the upward motions supply energy (22) which is carried toward the equator in the lower leg of the meridional cell. As a result the temperature increases ($\Delta T_\ell>0$) and forces the zonal wind component to increase ($U_{\ell-1}>0$) relative to the rigid shell component of superrotation. This is consistent with momentum transport in the lower leg of the meridional circulation which is balanced (24) by a divergence in the vertical momentum diffusion ($C_\eta>0$). Above the center of the meridional cell and above the tropopause ($S_o>0$), energy is carried away from the equator and the temperature decreases ($\Delta T_\ell<0$), forcing the zonal velocity to decrease ($U_{\ell-1}<0$) relative to the rigid shell component of superrotation. The poleward transport of momentum is again balanced by a convergence in the vertical momentum diffusion ($C_\eta>0$).

The picture portrayed here is somewhat simplified. In reality, the pressure increase due to thermal expansion in the troposphere extends upwards into the region which is convectively stable and thereby transports angular momentum to higher altitudes. Moreover, vertical diffusion of energy and momentum also contribute to couple the different regions. The result is that a complex interference pattern can develop such as we see it in the Jovian circulation.

For a net emitted flux of radiation, F_o, and given a vertical eddy diffusion coefficient K, the "stability" S_o at the pressure level p_o is estimated

$$S_o \equiv \left(\frac{\partial T_o}{\partial r} + \Gamma\right) = -\frac{kT_oF_o}{c_p p_o K}. \tag{26}$$

On Jupiter, $F_o = 1.5\times10^4$ ergs/cm^{2}sec (Orton and Ingersoll, 1976). Assuming $K = 10^6$ and $T_o = 170^o$, we derive a value of $S_o = -10^{-6}$ ^{o}deg/cm at the 1 bar pressure level which proves significant for the zonal circulation. Compared to Jupiter, Saturn is further away from the Sun and the net outward flux of radiation is smaller (R. Hanel, private communication). But, its troposphere appears to be less turbulent. Both effects would tend to compensate each other so that the superadiabatic lapse rate on Saturn may be comparable to that of Jupiter. On Venus, superadiabatic lapse rates have been inferred for the region between 50 to 60 km below the visible cloud top (Schubert et al., 1980) which, we believe, is important to understand the equatorial super-rotation on that planet (Mayr and Harris, 1981).

Latitude Structure: To understand the nature of mode coupling affecting the latitudinal structure of the circulation, we discuss here a simplified analytical solution for the equations (22) through (24). This will also elucidate some of the important elements that distinguish the atmospheric circulations on Jupiter, Saturn and Venus.

For $q_\ell = 0$, we consider the homogeneous equations (22) through (24) and obtain the expression

$$\ell \sim \sqrt{\ell(\ell+1)} = \frac{r\omega m(1-\beta)}{h}\sqrt{-\frac{H}{kc_p S_o}\,\frac{\left(\alpha+\frac{\ell(\ell+1)}{r^2}\kappa_\theta + C_\kappa\right)}{\left(\frac{\ell(\ell+1)}{r^2}\eta_\theta + C_\eta\right)}\,\frac{V_\ell}{|V_\ell|}} \tag{27}$$

Ignoring radiative cooling and assuming $(\frac{\ell(\ell+1)}{r^2}\kappa_\theta + C_\kappa)/(\frac{\ell(\ell-1)}{r^2}\eta_\theta + C_\eta) = \frac{c_p}{m}$, the coupling coefficient can be estimated

$$\beta \sim 1 - \frac{\ell h}{r\omega}\sqrt{-\frac{V_\ell}{|V_\ell|}\frac{g}{T_o}S_o} \tag{28}$$

For small ℓ values, near the fundamental mode where solar energy is deposited, momentum coupling is most effective; the "slippage" between the meridional velocity components of adjacent modes is small, and the value for β is close to one. Conversely, with $\beta \to 0$, mode coupling becomes small and a characteristic wave number R can be defined, which is a measure for the range over which momentum cascades

$$R \sim \frac{r\omega}{h}\sqrt{-\frac{V_\ell}{|V_\ell|}\frac{T_o}{gS_o}} \quad . \tag{29}$$

We consider the lower leg of the meridional circulation with $V_\ell < 0$ and $S_o < 0$. Adopting h=100 km, $T_o = 170^o$ and $S_o = -10^{-6}$ for Jupiter, one obtains R=28 and a characteristic latitude structure of $\lambda = \frac{360^o}{R} = 12^o$, in reasonable agreement with observations (Smith et al., 1979a,b). For Saturn, the gravitational acceleration as well as the planetary radius and rotation rate are smaller than for Jupiter. If we assume that on both planets the temperatures and the superadiabatic temperature lapse rates are about the same at the cloud level, this yields R = 14 or $\lambda = 24^o$, consistent with the Voyager measurements (Smith et al., 1981). The atmosphere of Venus is more compressed and we assume h = 10 km. Adopting an atmospheric rotation period on the order of 10 days and $S_o = -10^{-6}$, we obtain R = 4 or $\lambda = 90^o$; the circulation has global scale character, in substantial agreement with observations (Schubert et al., 1980).

The Equations (22) through (24) may serve to estimate the fundamental mode or the rigid shell component of superrotation

$$V_2 = \frac{-C_\eta \frac{\sqrt{6}}{r} \frac{k}{H} kq_2}{C_\eta \frac{6}{r^2} \frac{mgh}{T_o} c_p\, S_o + (\alpha + \frac{6}{r^2} \kappa_\theta + C_\kappa)\, \omega^2 m^2 (1-\beta)} \tag{30}$$

$$U_1 = \frac{\omega m}{C_\eta} |V_2| \tag{31}$$

$$\Delta T_2 = \frac{r\omega m H(1-\beta)}{\sqrt{6}kh} U_1 \quad . \tag{32}$$

Considering mode coupling in (24) due to $V_{\ell-2}$, and taking V_2 from (31), the solution for the higher order modes ($q_\ell = 0$, $\ell > 2$) can then be obtained in the form of simple recursion relationships given below.

$$V_\ell = \frac{\omega^2 m^2 (1-\beta)(\alpha + \frac{\ell(\ell+1)}{r^2} \kappa_\theta + C_\kappa) V_{\ell-2}}{\omega^2 m^2 (1-\beta)(\alpha + \frac{\ell(\ell+1)}{r^2} \kappa_\theta + C_\kappa) - \frac{\ell(\ell+1)}{r^2} \frac{mg}{kT_o} h^2 c_p S_o \frac{V_\ell}{|V_\ell|} (\frac{\ell(\ell-1)}{r^2} \eta_\theta + C_\eta)} \tag{33}$$

$$U_{\ell-1} = \frac{\omega m (V_{\ell-2} - V_\ell)}{(\frac{\ell(\ell-1)}{r^2} \eta_\theta + C_\eta)} \tag{34}$$

$$\Delta T_\ell = \frac{\omega m (1-\beta)}{\ell} \frac{Hr}{hk} U_{\ell-1} \quad . \tag{35}$$

The vertical velocity is given by (19), and the coupling coefficient β is defined with (27) or (28) in simplified form.

A more rigorous approach to the inhomogeneous ($q_2 \neq 0$) equations (22) through (24), without the need of a coupling coefficient β, would require a numerical solution that allows for momentum transfer over a wide range of modes. The order of this system would be limited by horizontal diffusion which dampens the amplitudes at rates proportional to $\frac{\ell(\ell-1)}{r^2}\kappa_\theta$ and $\frac{\ell(\ell+1)}{r^2}\eta_\theta$.

The analytical model (27) through (35) proves useful to gain some insight into the properties of atmospheric circulations. We present here an example representative of the conditions on Jupiter. Adopting $\omega = 1.8\times10^{-4}$, $S_o = \pm10^{-6}$, $m = 3.3\times10^{-24}$, $H = 100$ km and $K = 10^5$ and ignoring radiative cooling, results from the model are shown in Figure 8. Presented are the power spectra for the computed amplitudes of the zonal velocity, $U_{\ell-1}$, at the equator and their synthesis describing the latitudinal variations. It is assumed that under negative and positive stabilities, S_o, the meridional winds are directed toward the equator ($V_\ell>0$) and the poles ($V_\ell<0$) at lower and higher altitudes respectively. For positive values of C_κ and C_η, the expression under the radical (27) is then positive.

Compared to the fundamental mode or the rigid shell component of superrotation ($U_\ell>1$), which is driven primarily by the solar input ($q_2>0$), the indirect circulations driven by the momentum coupling with the lowest order mode are distinctly different. At lower altitudes where $S_o<0$, the indirect circulation contributes to equatorial superrotation. The amplitudes $U_{\ell-1}$, starting with $\ell = 4$, are significantly smaller than that of the fundamental mode and fall off gradually toward higher wave numbers (shorter wave lengths). This is in substantial agreement with the observations for $\ell < 18$ (Figure 1). In the synthesis of this spectrum a narrow equatorial jet is reproduced.

At higher altitudes with $S_o>0$, the direct circulation is again driven by differential solar heating which produces superrotation ($U_1>0$). However, the indirect circulation is now characterized by energy and momentum transport toward the poles. Starting with $\ell=4$ the zonal velocity components are negative and contribute to equatorial subrotation. Synthesizing this power spectrum, the result is that the atmosphere nearly corotates at the equator and superrotates at midlatitudes. The inclusion of horizontal diffusion and, partially, the truncation in our spectral analysis account for momentum transfer toward the equator at low latitudes which sustains a small superrotation rate.

Due to vertical convection and diffusion, the above discussed signatures from the upper and lower regions of the atmosphere are mixed, and we suggest that this is responsible for the complex circulation pattern observed on Jupiter. The observed negative equatorial velocity components around $\ell=22$ in Figure 1 may originate from a spectrum of the kind shown with the theoretical results in the lower part of Figure 5.

With the large rotation rate and large planetary radius of Jupiter, the second term in the denominator of (30) dominates. Assuming $\alpha=0$, the meridional velocity from (30) is $V_2 \propto q_2$, and the rigid shell component of superrotation from (31) is $U_1 \propto q_2/K$. Considering (28), (33) and (34), a trend analysis for the indirect circulation with $\ell>2$ gives

$$V_\ell \propto \frac{V_{\ell-2}}{1+\gamma\ell^2\sqrt{|S_o|}} \qquad (36)$$

$$U_{\ell-1} \propto \frac{\sqrt{|S_o|}\,V_\ell}{K}$$

where γ is an expression, usually positive, which involves atmospheric and planetary parameters. With increasing S_o a major component of the power spectrum is shifted toward lower wave numbers.

NUMERICAL RESULTS

We are demonstrating with this paper that in principle and contrary to current theories equational superrotation can be understood in the framework of a zonally symmetric circulation driven by solar differential heating. This suggests that the process is important for the large scale atmospheric motions observed on Jupiter and Saturn. To determine the extent that this is true will require a nonlinear analysis with general circulation models which account in self consistent form for the solar input and convective as well as radiative energy transfer. The results will depend on the vertical and horizontal eddy diffusivities and on the Prandtl number, and transport of latent energy is probably important.

Our discussion here is restricted to convey a general understanding of the mechanism. No attempt is made to simulate a particular planetary scenario.

For illustrative purposes a global average atmosphere is adopted which rotates at a rate of $1.8\times10^{-4}sec^{-1}$ in a gravitational field with g=2400 and is representative of the conditions on Jupiter. The data are based on the infrared measurements from the Voyager spacecraft (Hanel et al., 1979a,b). They are shown in Figure 9. Below the 1 bar pressure level, the temperature is extrapolated to lower altitudes assuming a (negative) stability $S_o = -5 \times 10^{-7}$ whose absolute value decreases toward lower altitudes satisfying flux continuity. The lower boundary is chosen to be at a pressure of 25 bar. Above the 2 mb level we assume the temperature to be constant. The upper boundary is chosen to be at a pressure of 5×10^{-11} bar where dissipative processes due to molecular diffusion dominate.

For the energy source driving the circulation, $\Delta q_2(r)$, we chose a height distribution shown in Figure 9 which was adopted from the work of Wallace et al., 1974. The specific heat input increases with height and accounts for the temperature inversion above the tropopause. Radiative cooling is considered in the form of a Newtonian coefficient $\alpha = 6.5 \times 10^{-6} p_o$ (ergs deg^{-1} $sec^{-1} gm^{-1}$) provided by B. J. Conrath (private communication). Vertical and horizontal eddy diffusion coefficients of 2.5×10^6 and 2.5×10^{11}, respectively, are chosen at the lower boundary and are assumed to increase with height at a rate inversely proportional to the square root of the density (Chapman and Lindzen, 1970).

We have used two different schemes to obtain solutions of the differential equations (9) through (13):

(1) Iterative Mode Coupling: With the heat source q_2, a solution of the fundamental mode ($\ell=2$) is obtained which describes a simple Hadley cell and the rigid shell component of superrotation (Mayr and Harris, 1981). The meridonal velocity in that mode couples momentum,through the Coriolis force, into the next higher mode (see the Equation (13) and the connection on the left hand side of the block diagram in Figure 6), and we obtain successive solutions for $\ell=4,6...$ Choosing some limiting wave number, we then turn around in our iteration procedure and consider the feedback due to momentum coupling by the zonal velocities (see Equation (12) and the connections on the right hand side of the block diagram in Figure 6), until we return to the fundamental mode of superrotation. The results substantially confirm our earlier conclusions. This solution procedure shows in particular that the feedback from the zonal velocity component in the higher wave numbers (shorter wavelengths) contributes to accelerate the equatorial region in the lower

order modes (longer wave lengths). Since the energy clearly comes from the heat source in the lowest order mode, our interpretation is that the feedback acts as a trapping mechanism. Under viscosity, velocity shears can numerically propagate in altitude, and the procedure eventually becomes unstable as one increases the number of iterations.

(2) Simultaneous Mode Coupling: With a limited number of 12 modes, momentum coupling is considered in self consistent form by simultaneously solving a system of 60 second order differential equations (egs. 9 through 13 for $\ell = 2$ to 24). The shortest wavelength covers about 15^{o} in latitude which is crude by comparison with the observed details in the Jovian circulation. It is again assumed that the lowest order heat source q_2 is driving the motions.

Results are shown for the zonal velocity and the relative temperature amplitude in the form of latitudinal distributions at various altitudes (Figures 10 and 11). The meridional circulation, of the Ferrel-Thompson type, is illustrated in Figure 12. One should expect that the dynamic properties of the atmosphere are sensitive to the tropospheric temperature lapse rates and the vertical and horizontal diffusivities as they vary with altitude. To understand the model fully and in relation to observations, will therefore require an extensive parametric analysis, the subject of a subsequent paper.

In the lower troposphere the temperature lapse rate is almost adiabatic. The meridional circulation does not extend all the way down but instead is broken up into smaller cells (Figure 12) which is reflected in the complex structure of the zonal wind field (Figure 10). Higher up, where a larger temperature gradient is required, $S_o \lesssim 5 \times 10^{-7}$, to conduct the heat from the planetary interior, the meridional circulation effectively focuses and traps energy and angular momentum in the equatorial region. A local temperature maximum (Figure 10) and a well defined equatorial jet thus develop at the equator. Very high up in the atmosphere where the temperature lapse rate is subadiabatic, heat is diffusing downwards and effectively disperses the energy that is transported upwards by the meridional circulation. As a result the latitudinal temperature distribution flatens and a blunt maximum develops at low latitudes where the solar energy is deposited (Figure 11). Moreover, angular momentum is carried to higher latitudes and broad maxima develop in the (eastward) zonal wind velocity. Due to upward convection in the form of thermal expansion from below and vertical as well as horizontal momentum diffusion, the equatorial region superrotates even at higher altitudes.

In the intermediate regions near 30 km, between the "dispersing" stable region above and the "focusing" unstable region below, the form of the zonal wind field resembles that of Jupiter. The horns near 10^{o} latitude are reproduced and secondary maxima develop near 30^{o} and 60^{o}. Lower down well within the unstable convection region at -20 km, the equatorial jet is larger by more than a factor of three and the form of the latitudinal velocity distribution resembles that of Saturn (Smith et al., 1981).

Based on this result we suggest that the large difference in magnitude between the equatorial jets of Jupiter and Saturn can in part be explained (Figure 13) by the temperature differences observed on both planets (Hanel et al., 1981). The clouds, which allow us to trace atmospheric motions, are formed on Jupiter near the tropopause where the transition occurs between two vastly different dynamic regimes one convectively stable the other one unstable. A complex interference pattern thus develops in the zonal circulation. On Saturn which is much colder, the clouds form at a much lower altitude, deep inside the convection region ($S_o < 0$) where the meridional circulation prevails in funneling energy and momentum into the equatorial region.

CONCLUSION

The important elements of the model are summarized in Figure 14. On Jupiter and Saturn global scale convection carries energy from the interior toward higher altitudes where radiation to space becomes important. The tropospheric regions should therefore be convectively unstable with small superadiabatic lapse rates on the order of 10^{-6}deg/cm. Under this condition, the upward motions in the direct and indirect atmospheric circulations imposed by insolation can then supply dynamic energy for "localized" equatorial heating which in turn drives equatorial superrotation. Preferential solar heating at low latitudes induces the ordered structure in the atmospheric motions. The efficiency of this process is determined by the degree of turbulence in the troposphere, the energy conversion in the planetary interior and the radiative loss from the upper troposphere and stratosphere. Differences in these global properties and the relative location of the clouds may contribute to the large differences between the zonal velocity fields on Jupiter and Saturn.

Adopting a spectral model, the concept of mode coupling is used to describe differential rotation and equatorial superrotation in an atmosphere with zonal and meridional viscous stresses. Momentum is thereby allowed to cascade from lower order modes, which "absorb" most of the solar energy, to higher order modes. At altitudes above the center of the meridional circulation, where the specific heat input is relatively large and the atmosphere is convectively stable, angular momentum is effectively advected poleward, except near the equator where the meridional winds and the Coriolis force vanish and the horizontal momentum transport must be carried by horizontal diffusion (viscous flow). This causes the atmospheric rotation rate to decrease at low latitudes and increase at high latitudes relative to the rigid shell component of superrotation; inducing a tendency for the equatorial region to corotate. However, below the center of the meridional circulation and below the maximum energy input where the atmosphere tends to be convectively unstable, angular momentum (and energy) are advected from high to low latitudes, thus the equatorial region can be accelerated to the extent that equatorial jets develop. Again, near the equator, angular momentum must be carried by horizontal diffusion; the equatorial minimum in the angular velocity on Jupiter (Figure 2) being evidence for down gradient diffusion toward the equator. This picture is complicated by vertical energy and momentum diffusion as well as convection which can effectively extend the characteristic circulation signatures from the troposphere into the stratosphere or visa versa.

Our theoretical results suggest that four factors are important in understanding the structure of the zonally symmetric circulation on Jupiter and Saturn: (1) Their large planetary size and rotation rate produce through mode/momentum-coupling a multiple Ferrel-Thomson type circulation with upward motions at low latitudes. Differences in the gravitational acceleration as well as in the planetary radius and rotation rate of both planets significantly contribute to broaden the latitudinal structure of the zonal circulation on Saturn relative to Jupiter. (2) Energy from the interior is diffusing radially outwards and maintains a superadiabatic lapse rate. This provides the condition for trapping or focusing dynamic energy that is advected toward the equator in the lower leg of the meridional circulation. (3) The eddy diffusivity is sufficiently low to require large temperature and velocity gradients in the energy and momentum balances. A vertical eddy diffusion coefficient between 10^5 and 10^6 may produce the zonal velocities observed on Jupiter; but a smaller value is probably required to explain the zonal circulation on Saturn. (4) Since the clouds are the tracers of atmosphric motions, their location is very important. On Jupiter they occur near the tropopause, in the transition zone between convectively stable and unstable regimes, and a complex interference pattern develops in the zonal circulation. In the atmosphere of Saturn which is colder, the clouds occur lower down well within the unstable convection region where the meridional circulation prevails in funneling energy and momentum into the equatorial region. This in turn is conducive to the development of a strong equatorial jet.

Mayr et al., 1981 argue that the large scale circulation on Jupiter provides the order in the formation of the small scale circulation features such as the great red spot and the white and brown ovals. Thus a relatively simple picture emerges for the Jovian circulation. The energy Jupiter radiates to space must be transported upwards through the troposphere. If that transport is accelerated by the prevailing upward motions in the solar driven meridionial circulation, eastward jets develop such as observed in the equatorial region. But, if that vertical transport is impeded by the prevailing downward motions in the solar driven multicellular meridional circulation, the atmosphere "reacts" and tends to maintain the process through the development of hurricanes. Dynamically induced by solar differential heating, a beautifully simple and ordered latitudinal structure, with alternating "stability" and "instability", is imposed on the troposphere, to form alternating zonal strata where hurricances in the form of red, brown, and white ovals are "forbidden" and "permitted", respectively.

Acknowledgements

We are deeply indepted to B. J. Conrath for many valuable discussions and for providing us with input data on the Jovian atmosphere, to R. Hanel, R. E. Hartle and K. Maeda for helpful comments, and to F. Varosi (Computer Science Corporation) for his assistance with the empirical analysis of the Voyager data.

References

Alexander, A. F. O.'D, The Planet Saturn, Faber and Faber, London, 1962.

Chapman, S., and R. S. Lindzen, Atmospheric Tides, D. Reidel Publ. Co., Dordrecht-Holland, 1970.

Conrath, B. J. et al., Atmospheric and surface properties of Mars obtained by infrared spectroscopy on Mariner 9, J. Geophys. Res., 78, 4267, 1973.

Gierasch, P. J., Meridional circulation and maintenance of the Venus atmospheric rotation, J. Atmos. Sci., 32, 1038, 1975.

Hanel, R. et al., Infrared observations of the Jovian system from Voyager I, Science, 204, 972, 1979a.

Hanel, R. et al., Infrared observations of the Jovian system from Voyager II, Science, 206, 952, 1979b.

Hanel, R. et al., Infrared observations of the Saturnian system from Voyager I, Science, 212, 192, 1981.

Held, I. M., and A. Y. Hou, Nonlinear axially symmetric circulations in a nearly invised atmosphere, J. Atmos. Sci., 37, 515, 1980.

Harris, I., and H. G. Mayr, Diurnal variations in the thermosphere: 1. Theoretical formulation, J. Geophys. Res., 80, 3925, 1975.

Hide, R., Motions in planetary atmospheres: A review, Meteor. Mag., 100, 268, 1971.

Hide, R., Dynamics of the atmospheres of the major planets with an appendix on the viscous boundary layer at the rigid boundary surface of an electrically conducting rotating fluid in the prescence of a magnetic field, J. Atm. Sci., 26, 841, 1969.

Ingersoll, A. P., Saturn's Atmosphere and Interior, EOS, 62, 254, 1981.

Ingersoll, A. P. et al., Zonal velocity and texture in the Jovian atmosphere inferred from Voyager images, Nature, 280, 773, 1979.

King-Hele, D. G., The rotational speed of the upper atmosphere determined from changes in satellite orbits, Planet. Space Sci., 12, 835, 1964.

Leovy, C. B., Rotation of the upper atmosphere of Venus, J. Atmos. Sci., 30, 1218, 1973.

Lorenz, E. N., The nature and theory of the general circulation of the atmosphere, World Meteorological Organization, 1967.

Mayr, H. G. and I. Harris, The rigid shell component of superrotation in planetary atmospheres: Angular momentum budget, mechanical analogy, and simulation of the spin up process, submitted to Plan. Space Sci., 1981 also Bull. Am. Astr. Soc., 12, 722, 1980.

Mayr, H. G., I. Harris, and N. W. Spencer, Some properties of upper atmosphere dynamics, Rev. Geophys. Space Phys., 16, 539, 1978.

Mayr, H. G., and H. Volland, Theoretical model for the latitude dependence of the annual and semiannual variations, J. Geophys. Res., 77, 6774, 1972.

Mayr, H. G., K. Maeda and I. Harris, On the global circulation and the hurricane system of the Jovian atmosphere, submitted to Planet. Space Sci., 1981.

Mayr, H. G., and I. Harris, Axisymmetric circulation and equatorial superrotation in planetary atmospheres, to be presented at the International Conference on the Venus Environment, Moffett Field, Ca., Nov. 1-6, 1981.

Morse, P. M., and H. Feshbach, Methods of Theoretical Physics, McGraw-Hill Book Co., New York, 1953.

Morrison, D., and J. Samz, Voyage to Jupiter, NASA-publication SP-439, 1980.

Orton, G. S., and A. P. Ingersoll, The thermal structure and H_e - H_2 ratio, Jupiter, University of Arizona Press, Tucson, Arizona, 1976.

Schubert, G. et al., Structure and circulation of the Venus atmosphere, submitted to J. Geophys. Res., 1980.

Smith, B. A. et al., Encounter with Saturn: Voyager I imaging science results, Science, 212, 163, 1981.

Smith, B. A. et al., The Jupiter System through the eye of Voyager I, Science, 204, 951, 1979a.

Smith, B. A. et al., The Galilean satellites and Jupiter: Voyager I imaging science results, Science, 206, 921, 1979b.

Volland, H., and H. G. Mayr, A three-dimensional model of thermospheric dynamics, 1, Energy sources and eigen functions, J. Atm. Terr. Phys., 34, 1725, 1972a.

Volland, H., and H. G. Mayr, The degeneration of Hough functions within the thermosphere, Space Res., 12, 1095, 1972b.

Wallace, L., P. Michael and M.J.S. Belton, The thermal structure of the atmosphere of Jupiter, Astroph. Journal, 193, 481, 1974.

FIGURE CAPTIONS

Figure 1: Empirical model of the zonal wind velocities observed from the Voyager spacecraft (G. Hunt, private communication) in terms of vector spherical harmonics which are used as basis functions in the subsequent theoretical analysis. Data from both hemispheres are taken, but only the terms symmetrical with respect to the equator are presented (lower part) and considered for the syntheses. Syntheses up to wave number L = 12 and 34 are shown (upper part). The rigid shell component (ℓ=2), directly driven by solar differential heating, dominates, and the lower order terms reproduce the equatorial jet. Note the simple form of the power spectrum; the Voyager I and II data being nearly identical.

Figure 2: The zonal wind field based on Voyager and Earth based measurements is taken from the NASA publication Voyage to Jupiter (Morrison and Samz, 1980) and shows a minimum below 7° latitude, indicative of downgradient diffusion toward the equator. We consider an equatorial region (right side) in which the angular momentum budget is established with horizontal and vertical diffusion. Thus, a priori, there is no constraint on the direction or magnitude of the zonal velocity at the equator and the question reduces to how angular momentum is effectively transported into the equatorial region?

Figure 3: Schematic illustration of the mass (top)-and momentum (bottom)-budgets for the direct circulation producing rigid shell superrotation which is observed on virtually every planet in our solar system. The balance is established between upward transport of momentum by convection (more being carried upwards at low latitudes than is carried downwards at high latitudes)

and diffusion. During "spin up" the atmosphere receives the angular momentum for superrotation from the planet or the planetary inferior.

Figure 4: Relative to the rigid shell component of superrotation (dashed lines), angular momentum is redistributed by the indirect circulation within the atmosphere. The momentum transport is toward the poles in the upper leg of themeridional cell thus increasing the superrotation at mid latitudes (plus sign) and decreasing it near the equator (minus sign). In the lower leg of the meridional circulation this process is reversed; angular momentum is redistributed toward the equator and an equatorial jet can develop (plus sign) under certain conditions (See Figure 5). It is thereby understood that in the equatorial region the horizontal momentum transport is taken over by horizontal diffusion (Figure 2).

Figure 5: Ignoring the added complexity due to horizontal diffusion, the momentum balance between horizontal advection and vertical diffusion is schematically illustrated. The equator is understood to be the equatorial region. Three different height distributions satisfy the budget. Case (a) is illustrated in Figure 4. In cases (b) and (c) the atmosphere superrotates and subrotates at all altitudes. The outcome depends on the energy budget illustrated in the lower part. To sustain equatorial superrotation the meridional circulation must accumulate energy at the equator. The condition for this arises when the atmosphere is convectively unstable, $S_o = (\frac{\partial T_o}{\partial r} + \Gamma) < 0$, which is presumably satisfied in the tropospheres of Jupiter and Saturn.

Figure 6: **Block diagram illustrating the mode/momentum coupling for the spectral model. The heat source in the fundamental mode, q_2, is directly driving the rigid shell component of superrotation. Mode coupling through the solenoidal (meridional) velocity field in turn is driving the indirect circulation by cascading momentum from lower to higher order modes (left hand side of the chain link). A feedback through the solenoidal or zonal velocity field (right side of the chain link) tends to trap angular momentum in the lower order modes.**

Figure 7: Heuristic discussion of various scenarios for the zonal velocity field in the equatorial region based on the equations (22) through (24). An equatorial heat source is forcing upward motions and equatorward and poleward winds in the lower and upper legs of the meridional circulation, respectively. In the direct circulation a rigid shell component of superrotation is produced (a). Superimposed on that fundamental mode the indirect circulation produces differential rotation with zonal velocities at the equator illustrated in the upper part of Figure 7. The sum of the rigid shell component and differential rotation is shown in the lower part of Figure 7. Cases (b) and (c) represent conditions where the atmosphere is convectively stable and unstable, respectively. Under case (d) the atmosphere is unstable and stable in the lower and upper legs of the meridional circulation, respectively.

Figure 8: The analytical model (30) through (35) is used to describe the latitudinal distribution in the upper and lower legs of the circulation corresponding to case (d) in Figure 7. The power spectra are shown in the lower part; for this display the amplitudes of the indirect circulation are scaled by a factor of three. Considering (25) the solution represents local

conditions where the two altitude regimes are weakly coupled. When coupling is important near the transition from one to the other regime a complex interference pattern can develop such as observed on Jupiter where besides the equatorial jet eastward jets are also observed at higher latitudes.

Figure 9: Input data for the average temperature, T_o, and pressure, p_o, the vertical eddy diffusion coefficient, k, and the heat input, q_2. In the troposphere near the 1 bar pressure level, the (negative) stability is assumed to be $S_o = -5x10^{-7}$; its absolute value decreasing toward lower altitudes so that the heat flux is conserved.

Figure 10: Latitudinal velocity distributions at various altitudes obtained from a numerical solution of the theoretical model. Note the large equatorial jet at -20 km and the velocity maximum near 30^o at higher altitudes. In between a complex velocity field develops which has some resemblance with that of Jupiter.

Figure 11: Same as Figure 10 except that the relative temperature amplitude is shown. Note the sharp maximum at the equator at altitudes where the narrow eastward jet develops. At higher altitudes the maximum is very broad, indicative of poleward energy transport (adiabatic cooling) by the indirect circulation.

Figure 12: The meridional circulation, based on out theoretical results, is illustrated. We refer to it as a multicellular Ferrel-Thomson circulation.

Figure 13: Based on the results from Figure 10, we suggest that the observed differences in temperature between Jupiter and Saturn (Hanel et al., 1981) are in part responsible for the large differences between the velocity fields observed on both planets (Smith et al., 1981). On Jupiter, the clouds condense near the tropopause which is in a transition region between the stable and unstable convection regimes above and below, where poleward and equatorward transport dominate, respectively. Thus a complex interference pattern develops such as seen in Figure 10 at 20 km. On Saturn which is much colder, the clouds condense about 50 km lower well within the unstable convection regime. The lower leg of the meridional circulation thus dominates in funneling energy and momentum into the equatorial region, much like hurricanes are formed on a much smaller scale. This process is conducive to the development of a relatively large equatorial jet such as seen in Figure 10 at -30 km which is analogous to the conditions on Saturn.

Figure 14: The important elements of the model are summarized in schematic form. On average the troposphere is convectively unstable; a superadiabatic temperature lapse rate accomodates the upward transport of heat from the planetary interior which is radiated to space at higher altitudes. Above the tropopause the solar heat input dominates and energy is conducted to lower altitudes where collisional excitation permits reradiation. Against this "homogeneous" background, the atmosphere is preferentially heated by solar radiation at low latitudes which brings order into the large scale atmospheric motions, effectively polarizing them. Air is rising at the equator and falls at higher latitudes. Thus angular momentum from the vast reservoir of the planet is stored in the atmosphere during "spin up" causing it to superrotate on average (rigid shell component of superrotation). With the large rotation

rate and radius of the planet the Hadley circulation is broken up into a multicellular meridional circulation with alternating rising and falling motions in the troposphere. Under conditions which are convectively unstable, the upward motions, focused by the Coriolis force into narrow latitude regimes effectively funnel energy and momentum into the equatorial region, for example, which is conducive to the formation of an equatorial jet.

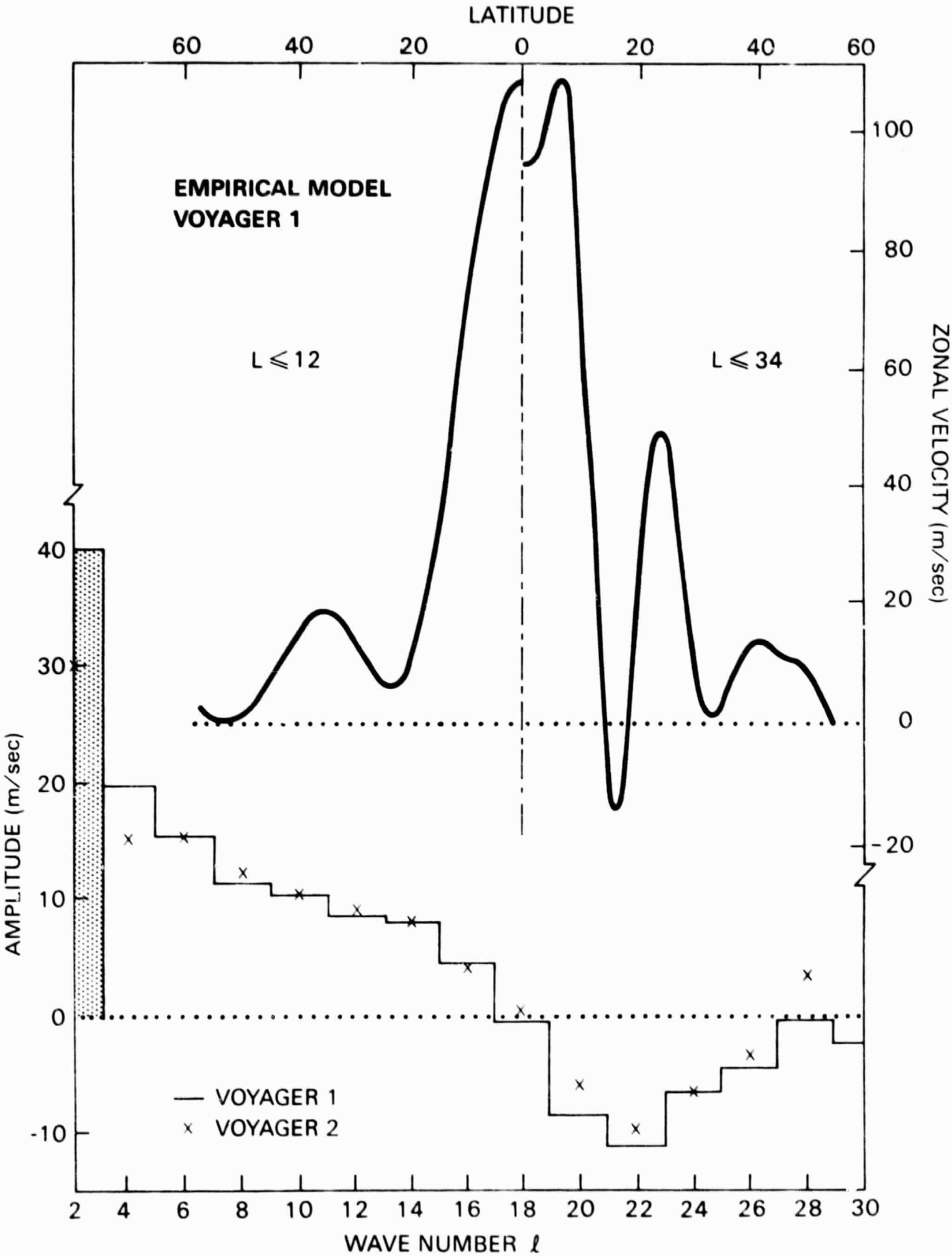

LATITUDE
60
40
20
0
20
40
60
EMPIRICAL MODEL
VOYAGER 1
L ≤ 12
L ≤ 34
100
80
60
40
20
0
-20
ZONAL VELOCITY (m/sec)
AMPLITUDE (m/sec)
40
30
20
10
0
-10
— VOYAGER 1
× VOYAGER 2
2
4
6
8
10
12
14
16
18
20
22
24
26
28
30
WAVE NUMBER ℓ

Figure 1

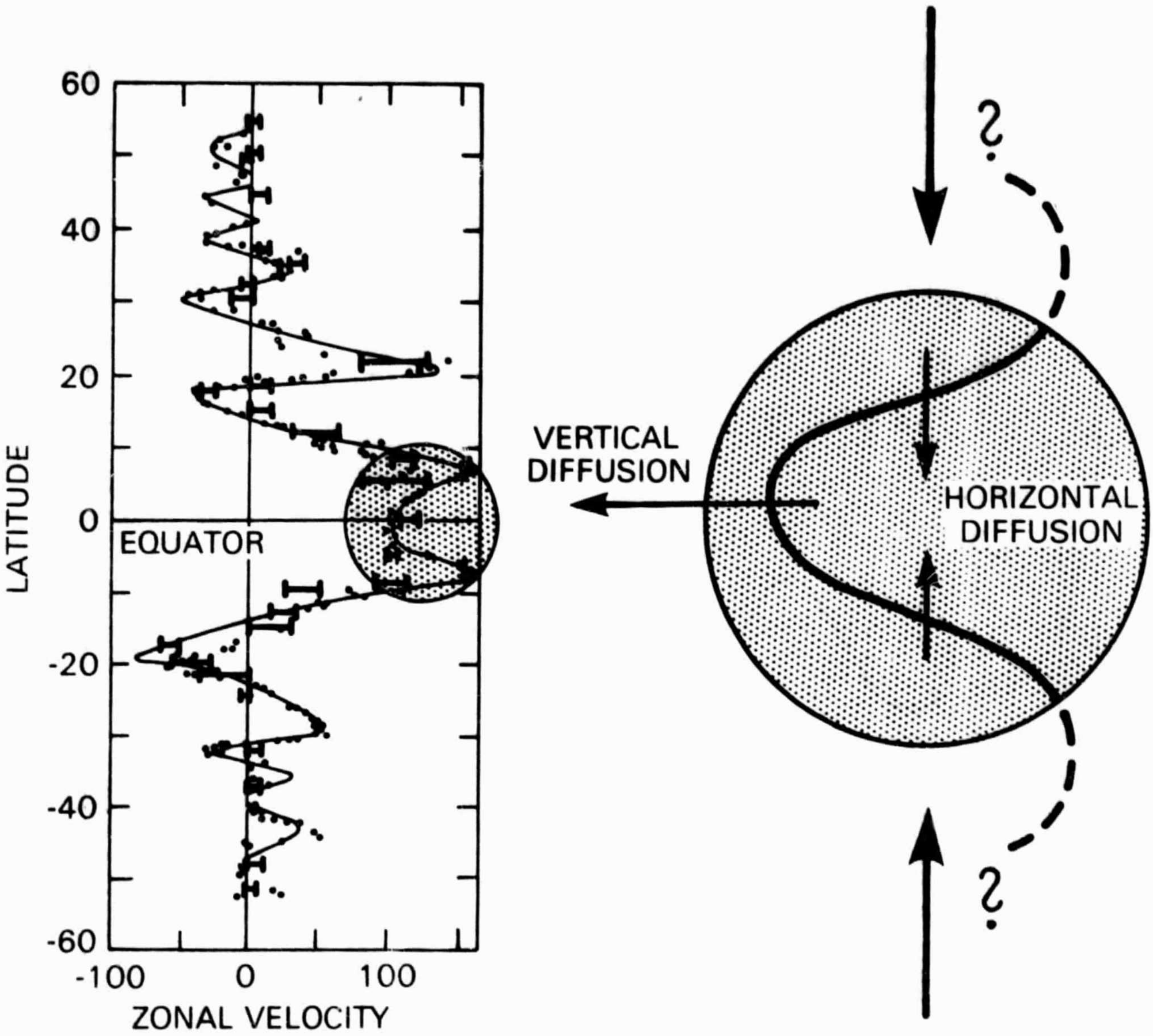

60
40
20
0
-20
-40
-60
LATITUDE
EQUATOR
-100
0
100
ZONAL VELOCITY
VERTICAL
DIFFUSION
HORIZONTAL
DIFFUSION
?
?

Figure 2

DIRECT CIRCULATION:

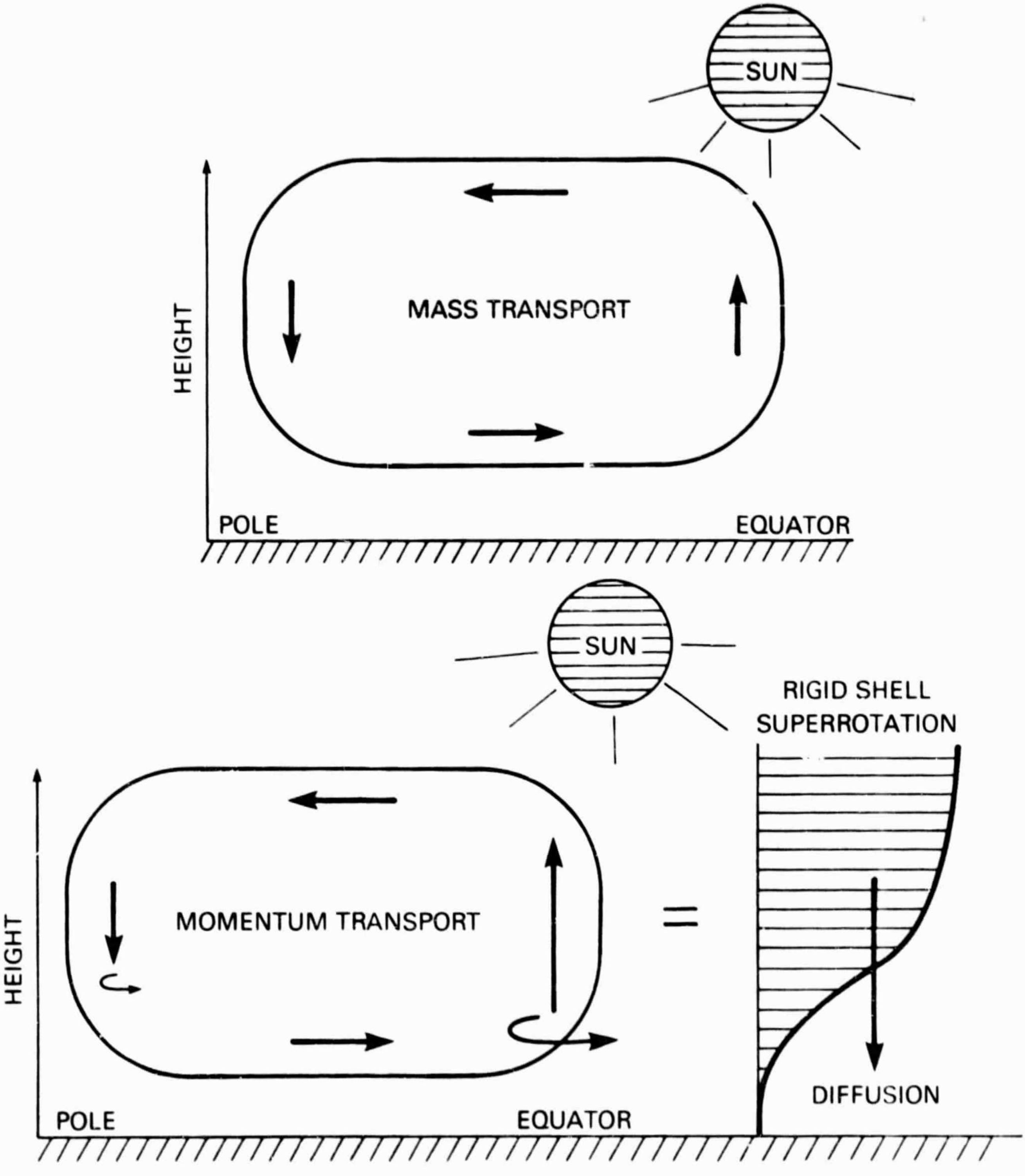

Figure 3

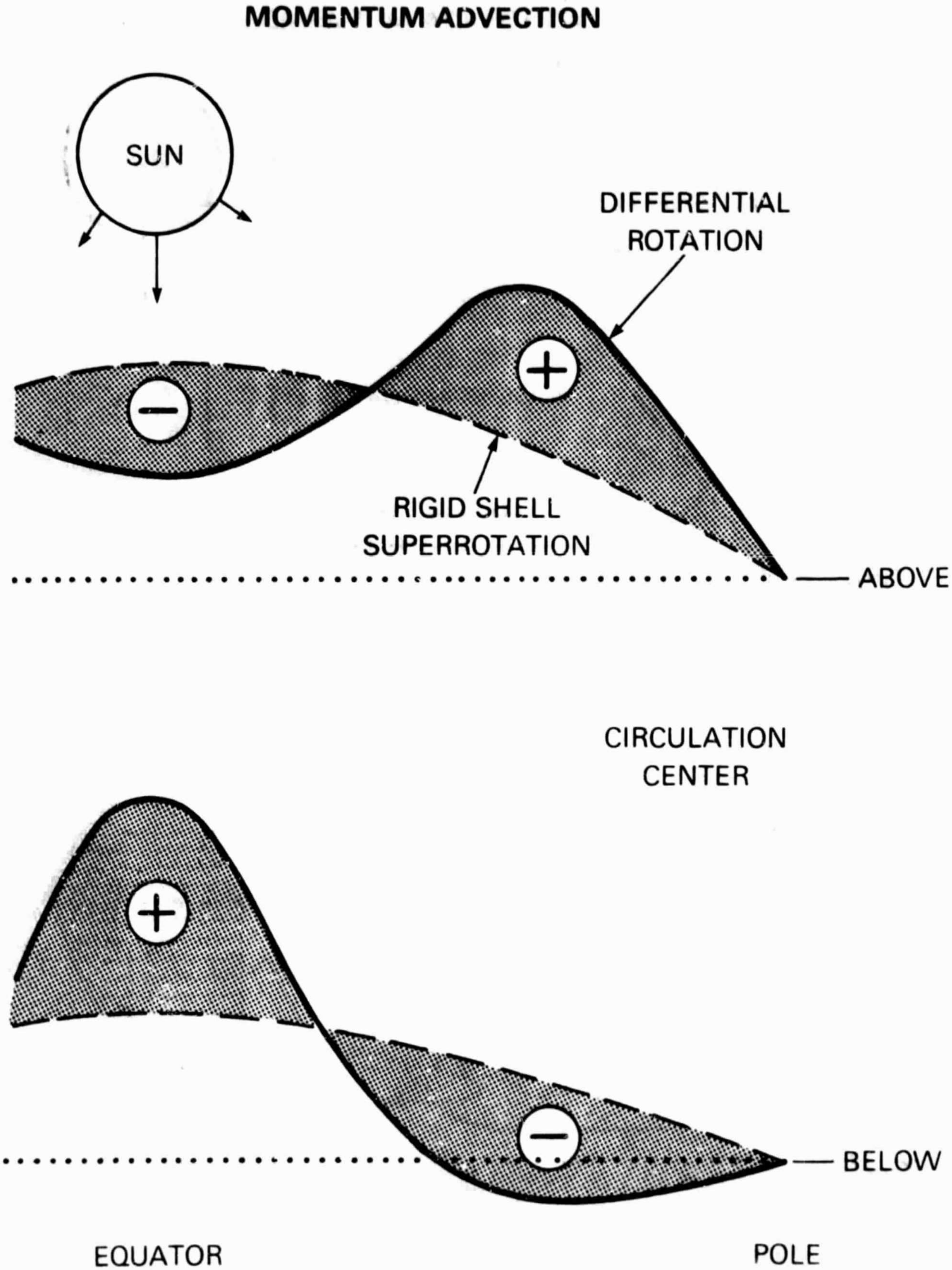
MOMENTUM ADVECTION
SUN
DIFFERENTIAL
ROTATION
RIGID SHELL
SUPERROTATION
ABOVE
CIRCULATION
CENTER
BELOW
EQUATOR
POLE

Figure 4

INDIRECT CIRCULATION:

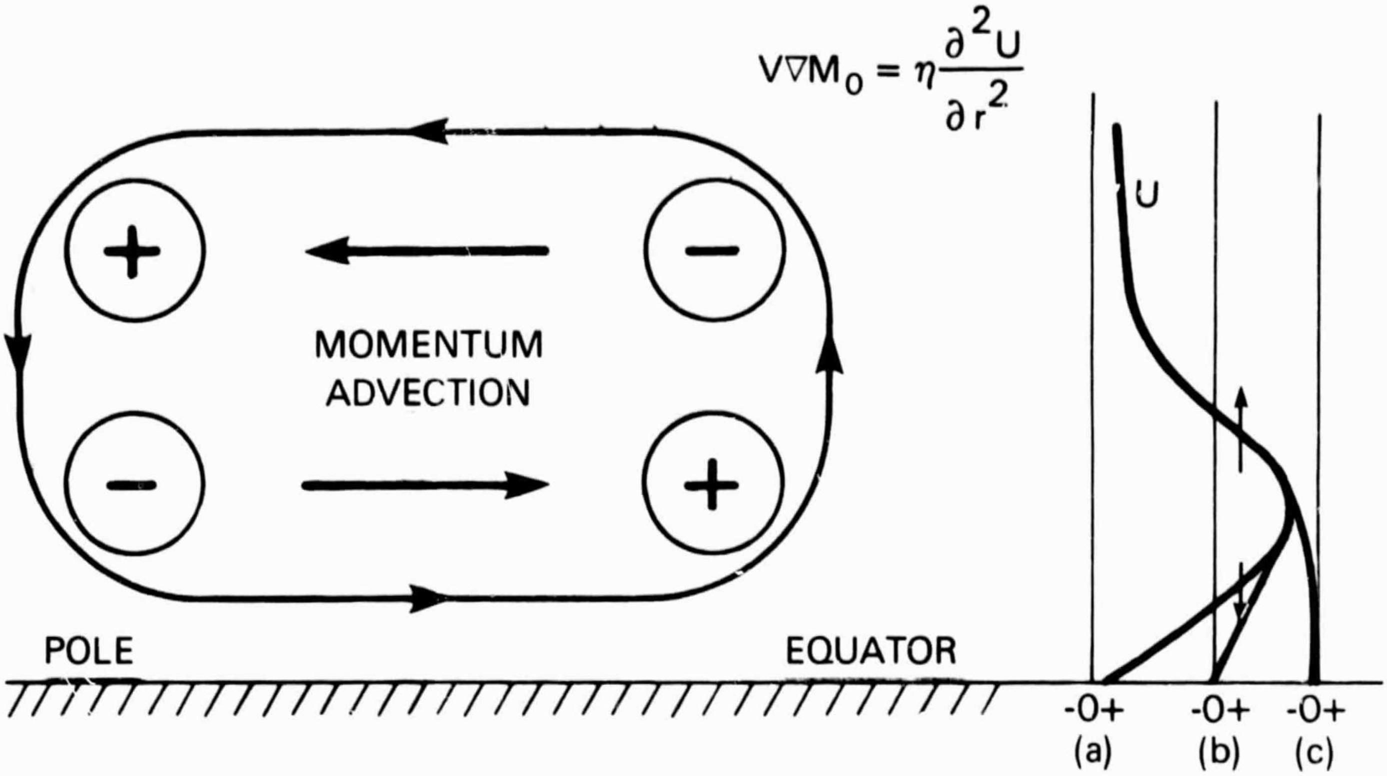

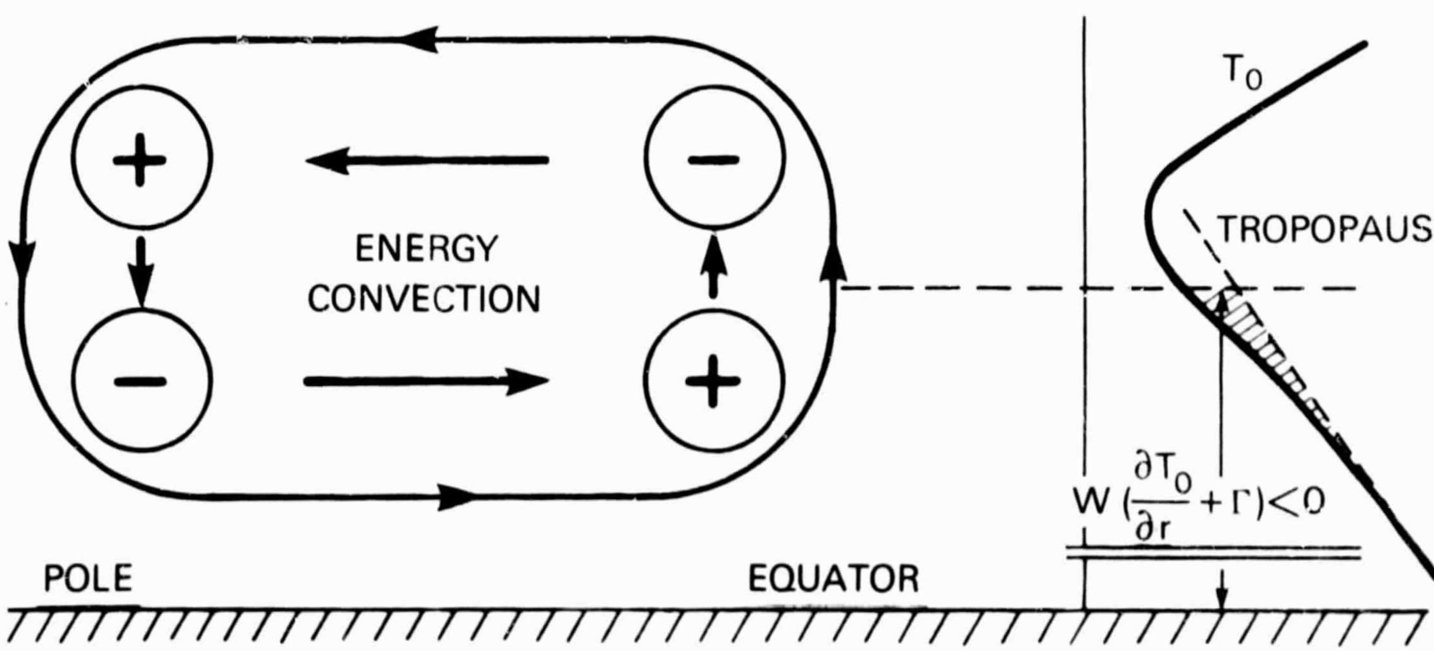

Figure 5

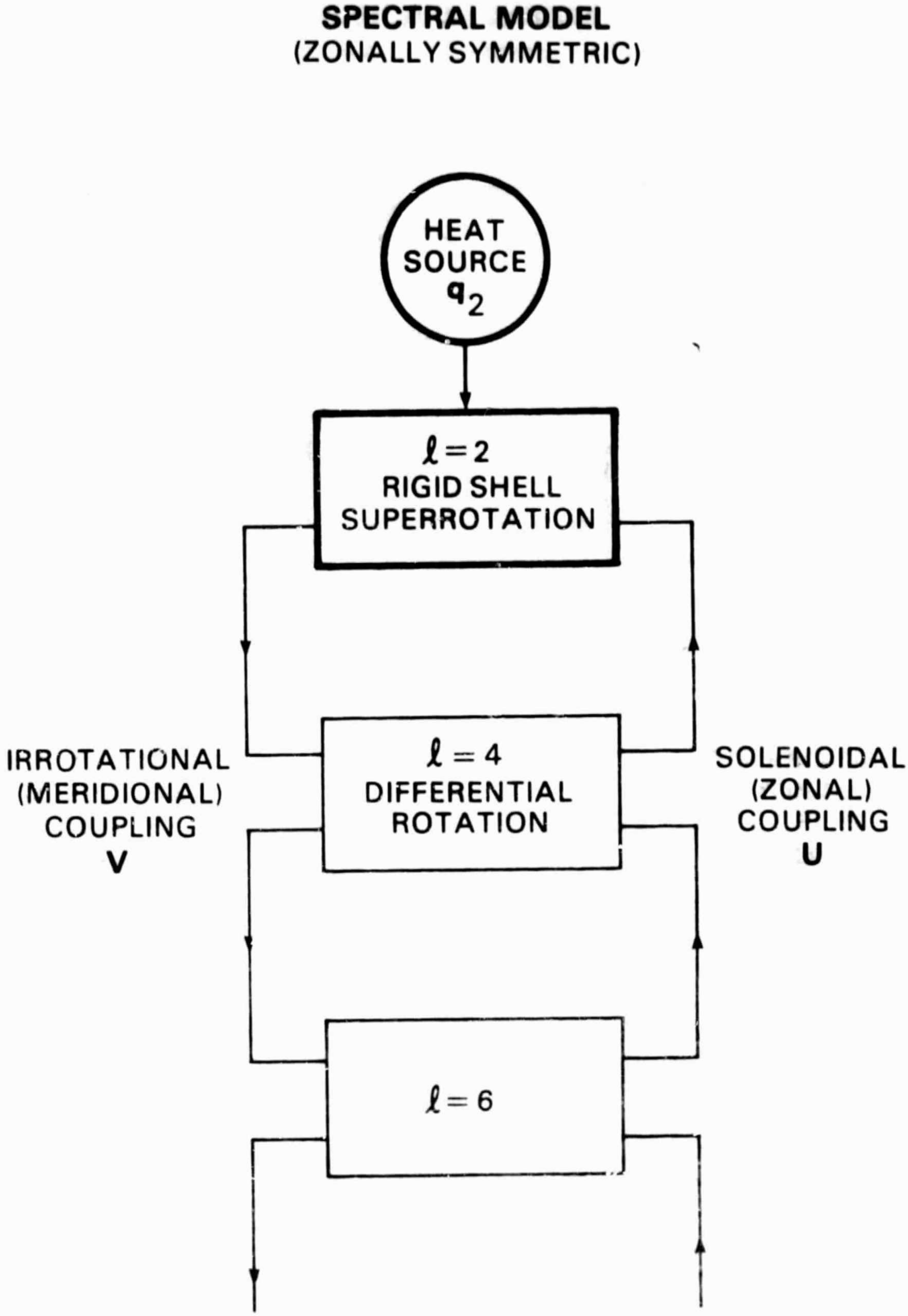
SPECTRAL MODEL
(ZONALLY SYMMETRIC)
HEAT SOURCE q_2
$\ell = 2$
RIGID SHELL SUPERROTATION
IRROTATIONAL (MERIDIONAL) COUPLING V
$\ell = 4$
DIFFERENTIAL ROTATION
SOLENOIDAL (ZONAL) COUPLING U
$\ell = 6$

Figure 6

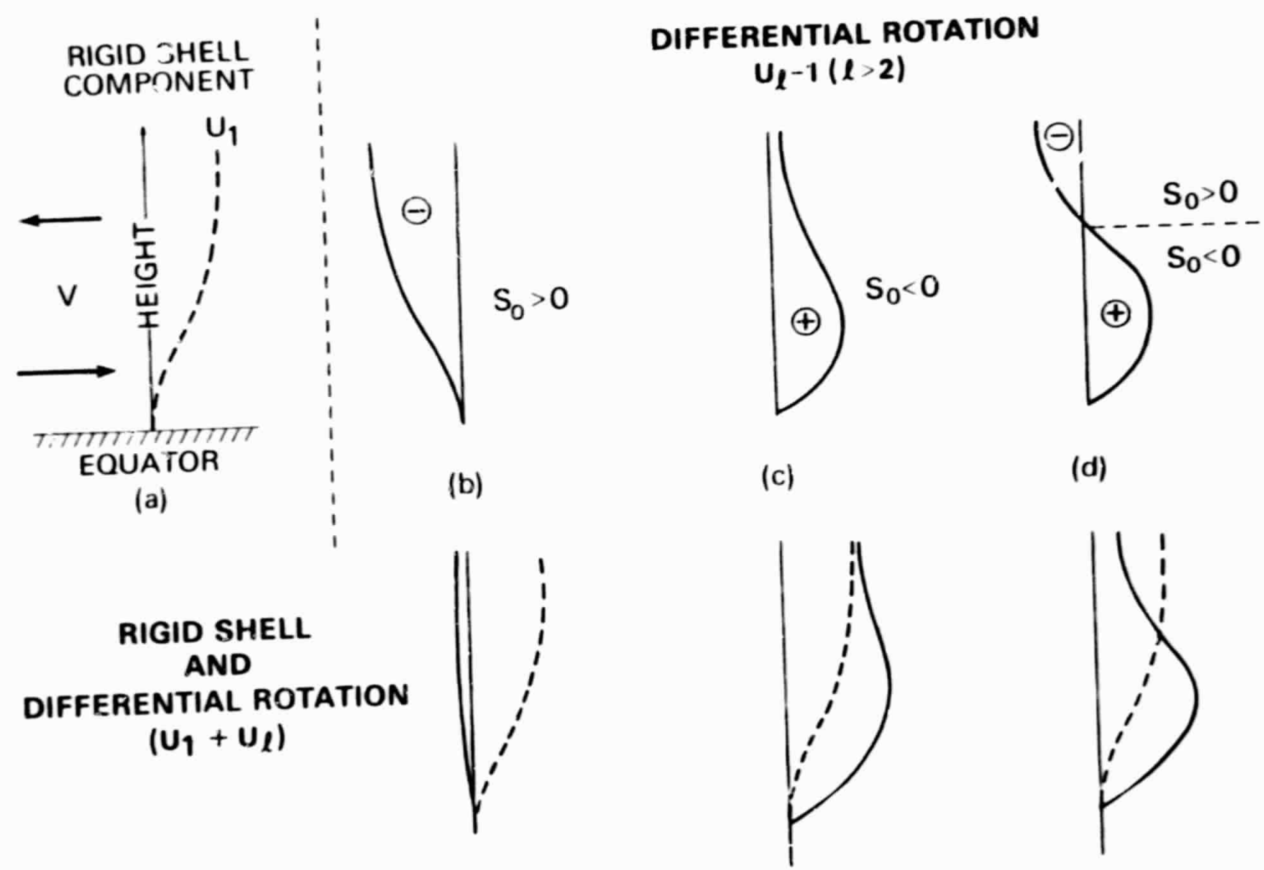

RIGID SHELL COMPONENT
U_1
HEIGHT
V
EQUATOR
(a)
DIFFERENTIAL ROTATION
U_ℓ-1 (ℓ>2)
$S_0>0$
$S_0<0$
$S_0>0$
$S_0<0$
(b)
(c)
(d)
RIGID SHELL
AND
DIFFERENTIAL ROTATION
($U_1 + U_\ell$)

Figure 7

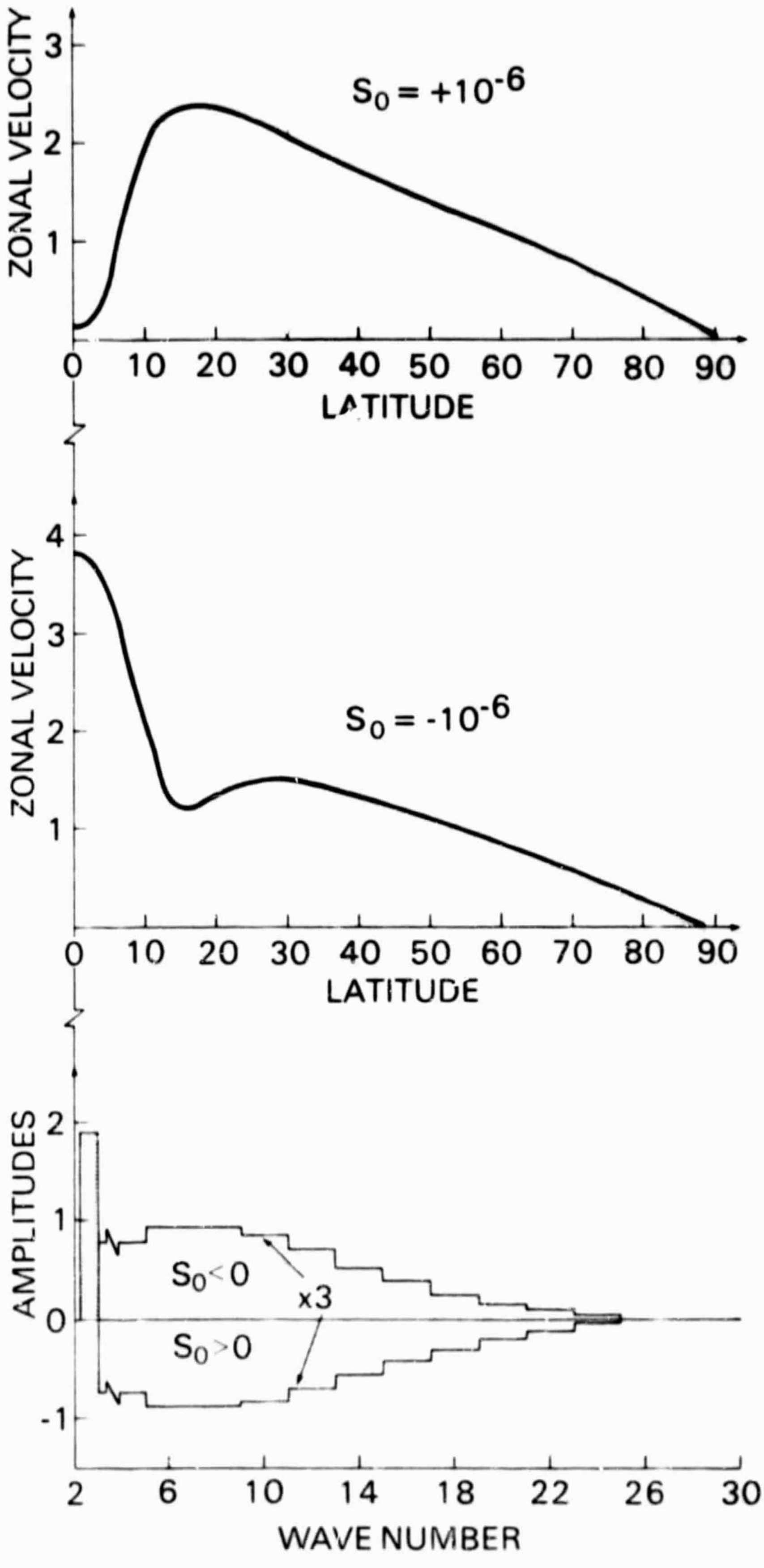

ZONAL VELOCITY
$S_0 = +10^{-6}$
LATITUDE
ZONAL VELOCITY
$S_0 = -10^{-6}$
LATITUDE
AMPLITUDES
$S_0 < 0$
x3
$S_0 > 0$
WAVE NUMBER

Figure 8

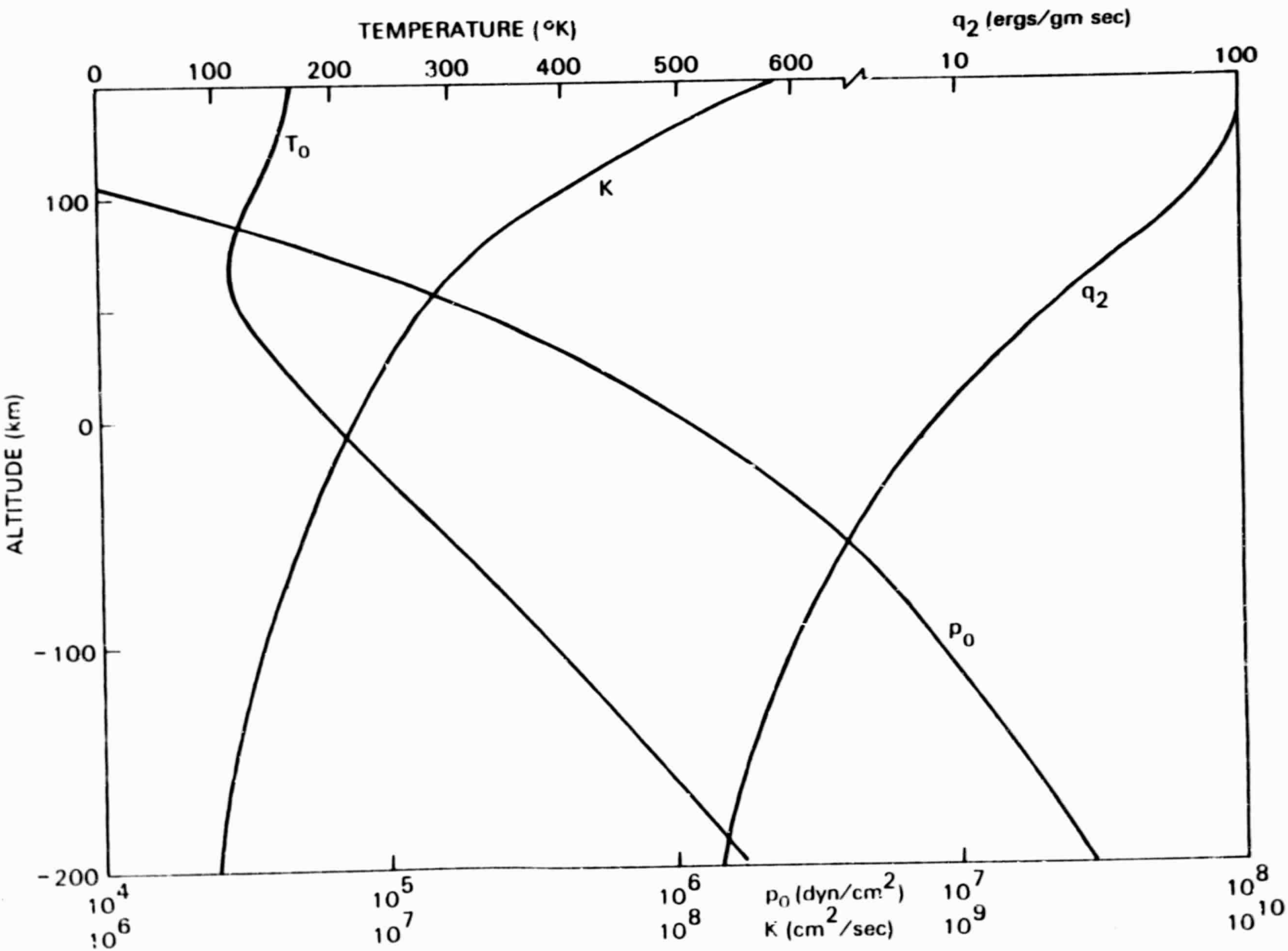
TEMPERATURE (°K)
0
100
200
300
400
500
600
q_2 (ergs/gm sec)
10
100
T_0
K
q_2
p_0
ALTITUDE (km)
100
0
-100
-200
10^4
10^6
10^5
10^7
10^6
10^8
p_0 (dyn/cm^2)
K (cm^2/sec)
10^7
10^9
10^8
10^{10}

Figure 9

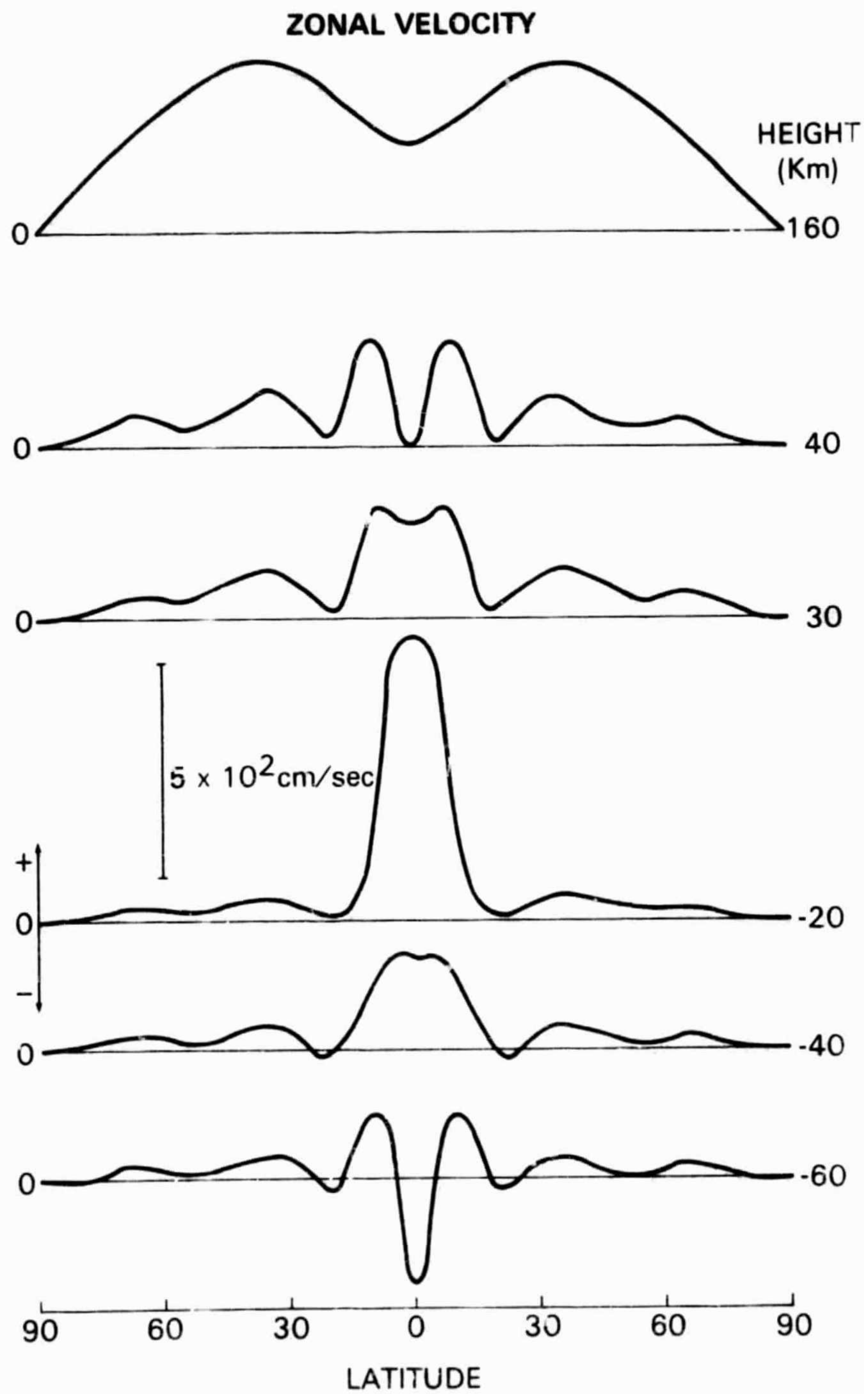
ZONAL VELOCITY
HEIGHT
(Km)
0
160
0
40
0
30
5 x 10^2cm/sec
+
0
-20
–
0
-40
0
-60
90
60
30
0
30
60
90
LATITUDE

Figure 10

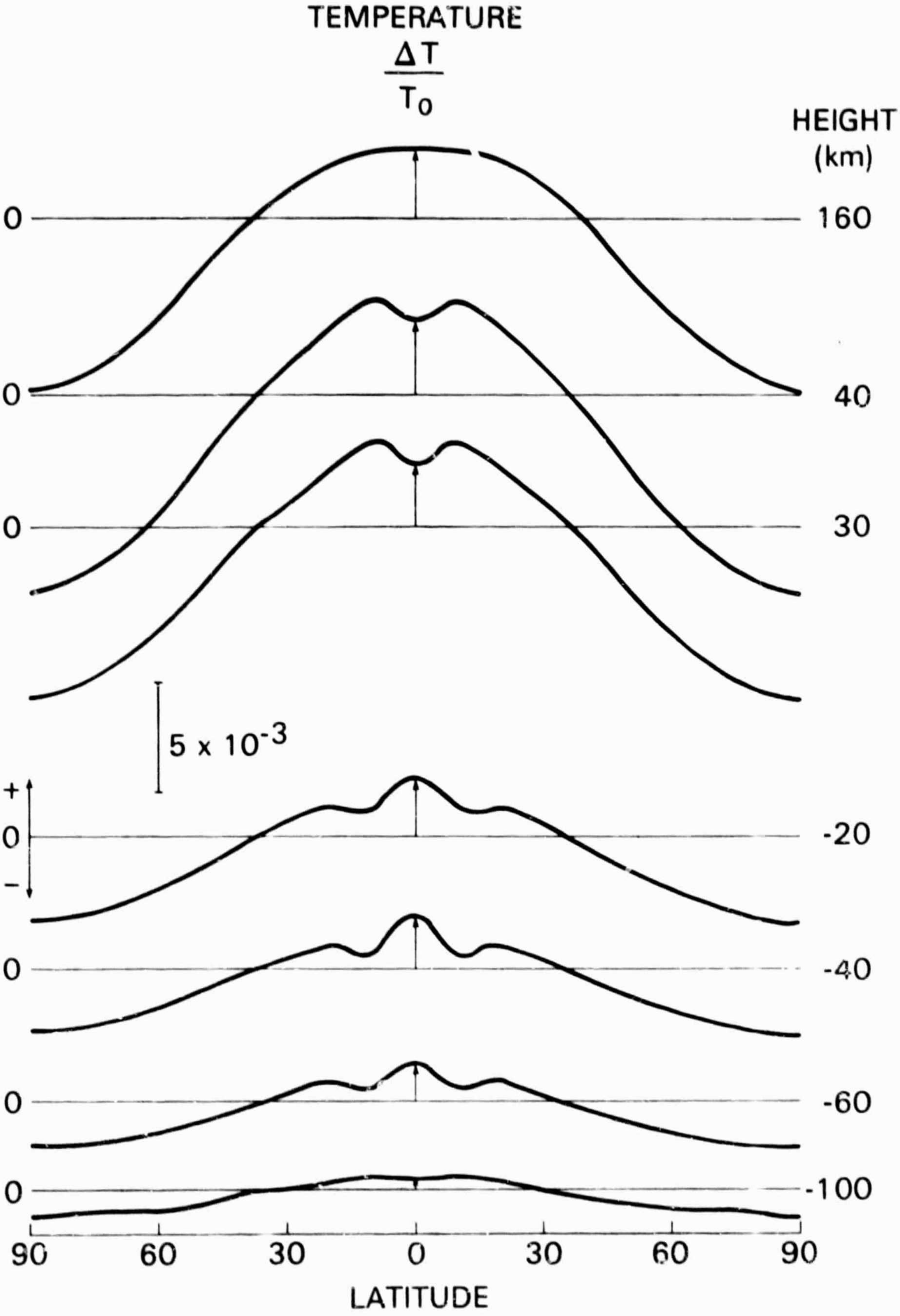
TEMPERATURE
$\frac{\Delta T}{T_0}$
HEIGHT
(km)
0
160
0
40
0
30
5×10^{-3}
+
0
−
-20
0
-40
0
-60
0
-100
90
60
30
0
30
60
90
LATITUDE

Figure 11

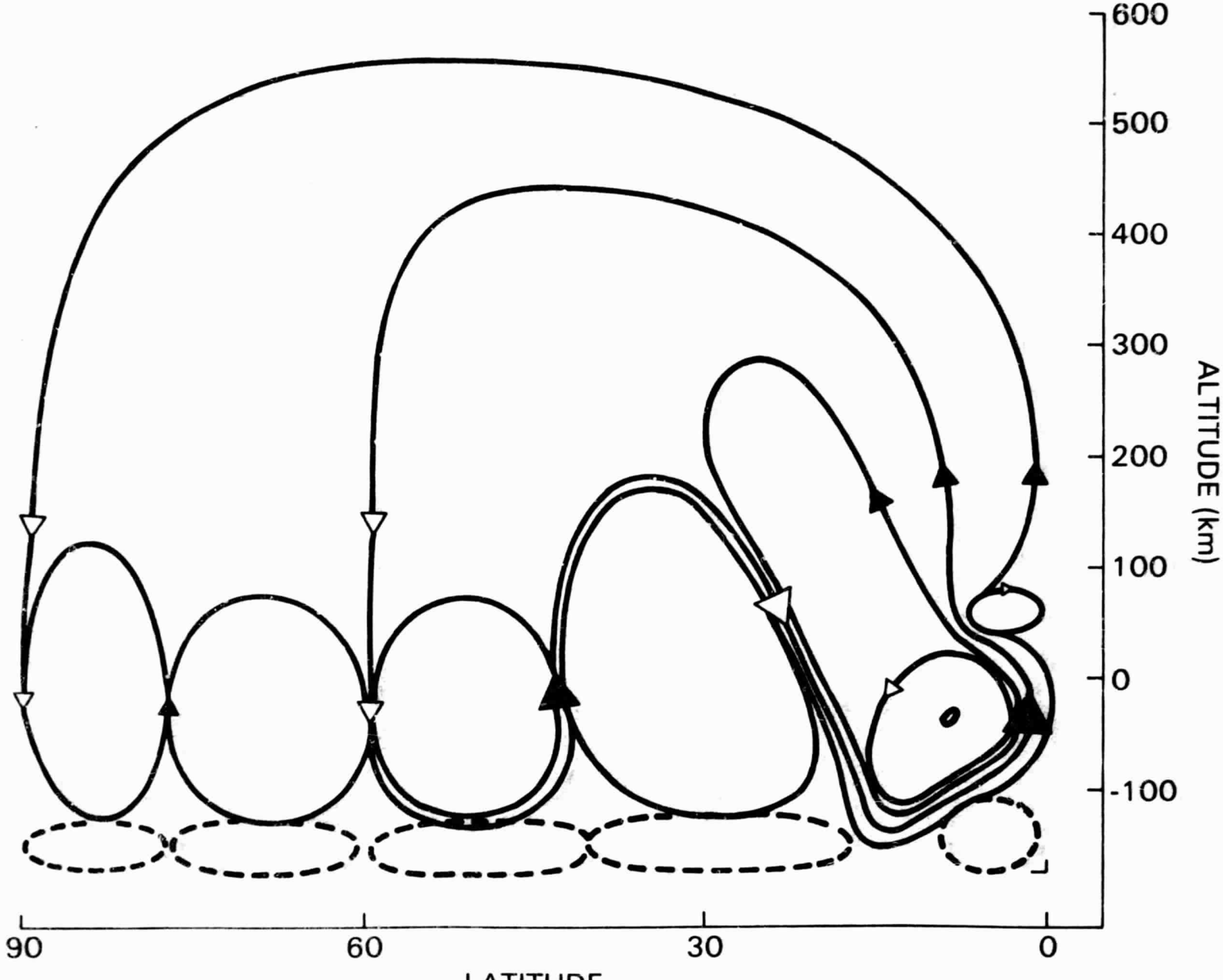

Figure 12

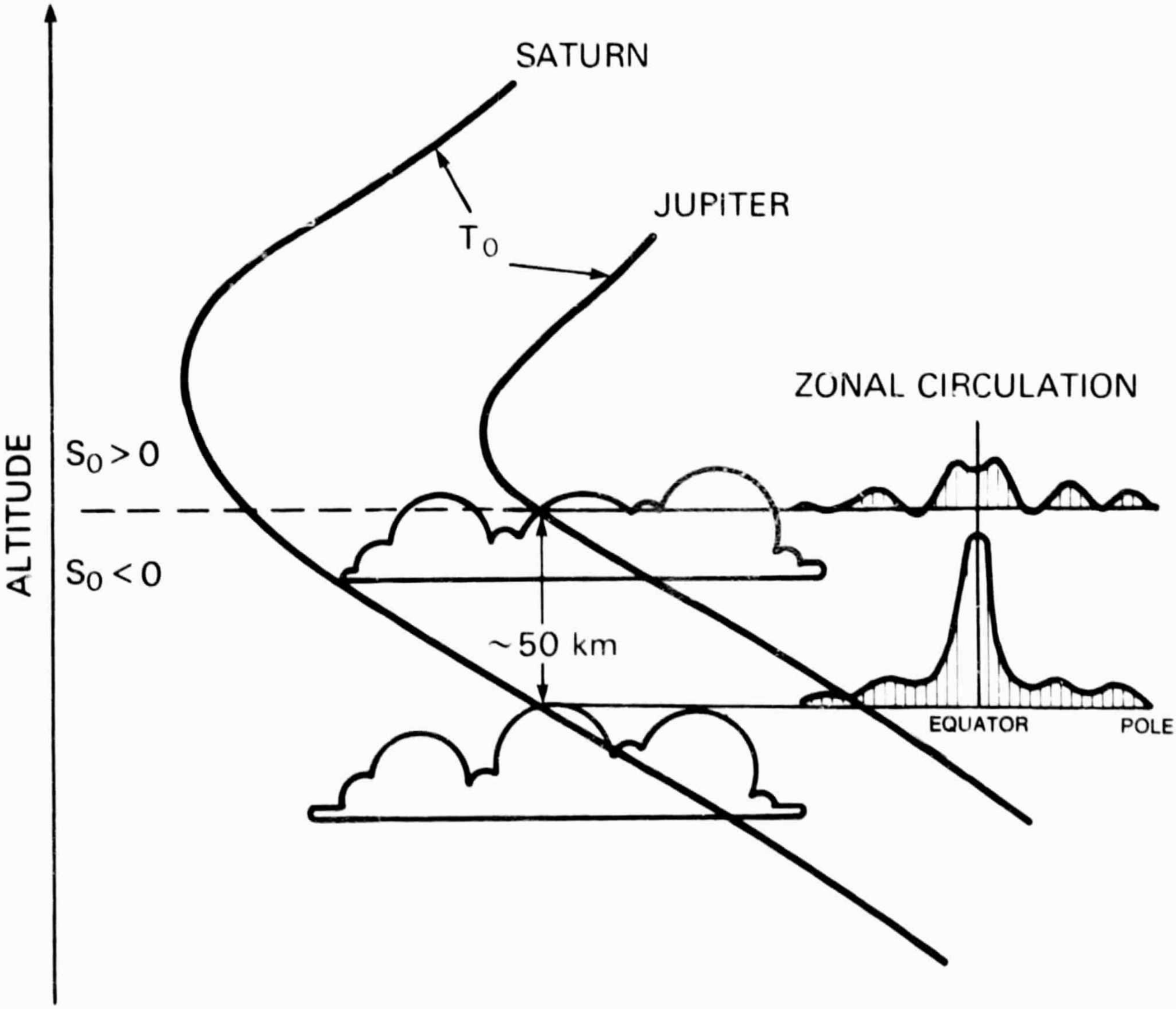

SATURN
JUPITER
T_0
ZONAL CIRCULATION
ALTITUDE
$S_0 > 0$
$S_0 < 0$
~50 km
EQUATOR
POLE

Figure 13

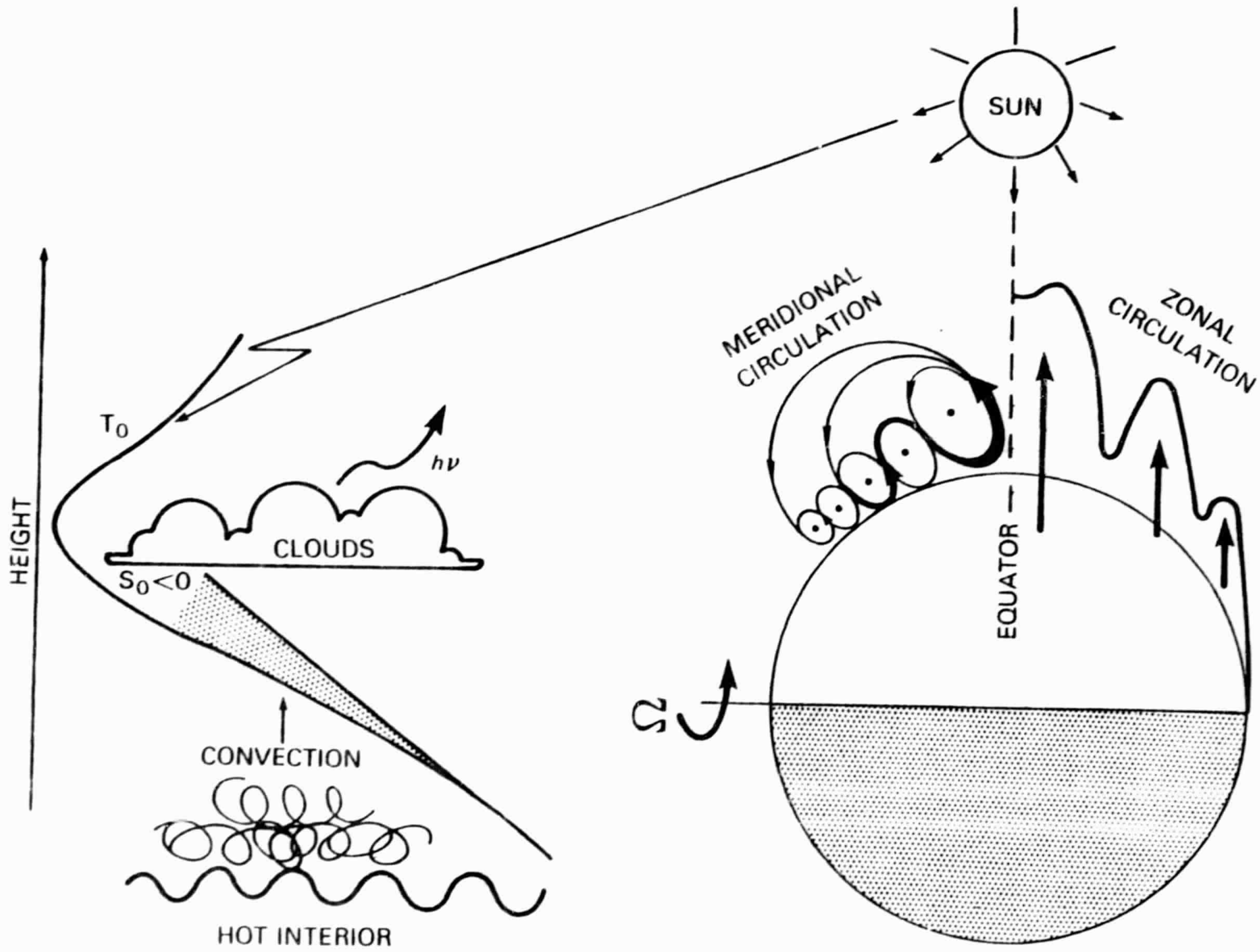
SUN
HEIGHT
T_0
$h\nu$
CLOUDS
$S_0<0$
CONVECTION
HOT INTERIOR
MERIDIONAL
CIRCULATION
ZONAL
CIRCULATION
EQUATOR
Ω

Figure 14